

**Application of Hansen Solubility Parameters in Fabrication of Molecularly Im-
printed Polymers for Detection of PAHs from Water Samples**

By

Maryam Jafari

A thesis submitted to the School of Graduate Studies in partial fulfillment of the require-
ments for the degree of Master of Science

Department of Chemistry

Memorial University of Newfoundland and Labrador

July 2018

St. John's

Newfoundland and Labrador

Abstract

Molecularly imprinted polymers (MIPs) are smart polymers for selective recognition of target analytes. This work focuses on developing MIPs for aquatic contaminants, such as polycyclic aromatic hydrocarbons (PAHs) in seawater. MIPs are generally prepared with a monomer, cross-linker, template or pseudo-template, and solvent (porogen). As with most porous adsorbents, MIPs exhibit high surface area and porosity, controlled pore size and mechanical stability. It has been recognized that the solvent system plays a key role in the pore generation, influencing the shape, size and volume of pores in MIPs. Rather than taking a trial-and-error approach, Hansen solubility parameters (HSPs) are used in this work to develop a model to predict the suitability of porogen for the formation of MIP films with specified porosity. Hansen solubility parameters help to predict the thermodynamic compatibility of a porogen with the prepolymerization components, which is a good estimate of the propensity to form a polymeric network with required characteristics.

MIPs fabricated using the systematic method based on Hansen solubility parameters were combined with GC-MS to determine the concentration of naphthalene, fluorene, phenanthrene and pyrene in water samples. The porous MIPs were also used to extract and determine the concentration of PAHs in produced water which is a byproduct generated along with the production of oil and gas from on shore and offshore platforms.

This is the first report of a predictive model for porogen selection in the preparation of porous MIP monoliths.

Acknowledgments

I would like to thank my supervisor, Dr. Christina Bottaro, for giving me the chance to pursue my Master of Science degree in chemistry, and for all her patience, guidance and help to improve my thesis over the years. I would like to thank my colleague Ali Azizi for his advice on GC-MS method development. I would like to thank Linda Winsor for all her help in the C-CART. I would also like to thank everyone in the Bottaro research group for the help they provided in the lab.

Finally, I want to thank my friends and my parents for their love, support, and encouragement.

Table of Contents

Abstract	ii
Acknowledgments.....	iv
List of Figures	ix
List of Tables	xii
List of Symbols, Nomenclature or Abbreviations	xiii
List of Appendices	xvi
Chapter 1. Introduction and Literature Review	1
1.1 Introduction to synthesis of porous polymers	1
1.1.1 Macroporous copolymer networks	1
1.1.2 Techniques for fabrication of macroporous particulate polymers and monoliths	3
1.1.3 Formation of polymers with porous structures	5
1.2 Solubility parameters.....	8
1.2.1 Solvation process and the Hildebrand solubility parameters.....	9
1.2.2 Hildebrand and Hansen solubility parameters.....	11
1.2.4 Three-dimensional Hansen space	12
1.2.5 HSP determination of polymers	14
1.2.6 The general Hansen algorithm.....	16

1.2.7 Selection of pore-former solvent based on HSPs	19
1.3 Molecularly imprinted polymers (MIPs).....	20
1.3.1 Molecular imprinting strategy	21
1.3.2 Factors affecting molecular recognition in MIPs	22
1.3.3 Molecular imprinting approaches	26
1.4 Detection methods used with MIPs.....	29
1.4.1 Gas chromatography (GC).....	29
1.4.2 Gas chromatography-mass spectrometry (GC-MS)	31
1.5 An overview of produced water	32
1.5.1 Definition and source.....	32
1.5.2 Chemical composition of produced water	33
1.5.3 Regulations	35
1.6 Polycyclic aromatic hydrocarbons (PAHs)	36
1.6.1 Sources, classification and distribution of PAHs	37
1.6.2 Analytical methods for detection of PAHs.....	38
1.7 Research goals	40
Chapter 2. Theoretical and Experimental Methods for Selection of Porogen for MIPs Fabrication	42
2.1 Introduction	42

2.2 Determination of poly(methacrylic acid) HSP	43
2.2.1 Synthesis of cross-linked poly(methacrylic acid) (PMAA).....	43
2.2.2 Swelling test of Cross-linked PMMA	44
2.2.3 Computation of the HSP for PMAA and application for solvent suitability	47
2.3. Effect of porogen type on thin-film MIPs	50
2.3.1 Materials	50
2.3.2 Methods	51
2.3.3. Results and discussions	53
2.4 Conclusions	60
Chapter 3. Using MIPs for Extraction of PAHs from Water Samples	61
3.1 Introduction	61
3.2 Materials	64
3.3 Methods	65
3.3.1 Adsorption experiments.....	65
3.3.2 GC-MS Method	66
3.4 Results and discussion.....	67
3.4.1 MIP fabrication.....	67
3.4.2. Binding studies of MIP for PAHs.....	68
3.4.3. Evaluation of adsorption properties of PAHs onto MIPs	72

3.4.4. Analysis of real samples	78
3.5 Conclusions	82
Chapter 4 Conclusions and Future Work	83
4.1. Conclusions	83
4.2 Future work	84
5. References	86

List of Figures

Figure 1.1 Preparation of porous beads using the swelling and polymerization technique. Copyright 1992 Wiley-VCH[21]. a) Styrene (monomer), b) monodisperse particulate template, c) swollen template particles, d) porous beads.....	4
Figure 1.2 Example of preparation of macroporous polymer monoliths [23]. Copyright © 2002, Springer-Verlag Berlin Heidelberg	5
Figure 1.3 Three-dimensional Hansen space.	13
Figure 1.4 General flowchart of Hansen algorithm[2].....	18
Figure 1.5 Molecularly imprinted polymer fabrication.	21
Figure 1.6 Typical functional monomers used for fabrication MIPs.....	24
Figure 1.7 Formation of carbon centered radical by thermal decomposition of AIBN. ...	26
Figure 1.8 Non-covalent and covalent molecular imprinting approaches. Used with permission [77].	27
Figure 2.1 The effect of contact time on the percent swelling of PMAA.....	45
Figure 2.2 Hansen Space of PMAA. The red circle denotes the Hansen sphere for PMAA.	49
Figure 2.3 MIP components structures	50
Figure 2.4 MIP slides prepared using different porogenic solvents: a) acetonitrile (RED = 0.271), b) chloroform (RED = 0.875), c) benzyl alcohol (RED = 0.989), d) 1-octanol (RED = 1.014), e) methanol (RED = 1.246), f) toluene (RED = 1.394), g) 1-octanol and methanol (v/v 80/20) (RED = 0.998).	54

Figure 2.5(a-c). SEM image of MIP fabricated using a) toluene, b) benzyl alcohol and c) 1-octanol.	58
Figure 2.5(d,f). SEM image of MIP fabricated using d) 1-octanol/methanol (80/20 v/v) e) pore details and sizes of d.	59
Figure 3.1a Calibration curve for extraction of a) naphthalene in aqueous multi-PAHs solutions using MIPs and NIPs with analysis by GC-MS in SIM mode.	68
Figure 3.1(b,c) Calibration curve for extraction b) fluorene and c) phenanthrene in aqueous multi-PAHs solutions using MIPs and NIPs with analysis by GC-MS in SIM mode.....	69
Figure 3.1d Calibration curve for extraction d) pyrene in aqueous multi-PAHs solutions using MIPs and NIPs with analysis by GC-MS in SIM mode.....	70
Figure 3.2 Time-dependent adsorption of naphthalene, fluorene, phenanthrene and pyrene onto the MIPs in 100 mL of 10 µg/L each. Measured by GC-MS in SIM mode. Two replicates. Peak ratio: peak area of analytes/peak area of internal standard.	73
Figure 3.3 Binding of PAHs for MIPs and NIPs. Experimental conditions: V=100.0 mL; C ₀ =1 mg/L; mass of polymer=50 mg (used with permission from reference [150]).....	74
Figure 3.4(a,b) Freundlich binding isotherms graph for a) naphthalene and b) fluorene, adsorbed by for MIP/NIP uploaded in 100 mL of aqueous PAHs solution in 10-100 µg/L concentration range.	76
Figure 3.4(c,d) Freundlich binding isotherms graph for c) phenanthrene and d) pyrene adsorbed by for MIP/NIP uploaded in 100 mL of aqueous PAHs solution in 10-100 µg/L concentration range.	77

Figure 3.5(a,b) Calibration curve of a) naphthalene b) fluorene in produced water using standard addition method by GC-MS.	80
Figure 3.5(c,d) Calibration curve of c) phenanthrene d) pyrene in produced water using standard addition method by GC-MS.	81

List of Tables

Table 1.1 Controlling morphology of styrene-divinylbenzene by changing the solvation power of the porogen [30].....	7
Table 1.2 HSPs of some common solvents [34].	15
Table 1.3 Concentration ranges of natural organic chemicals in worldwide produced water [99].	34
Table 1.4 Daily maximum and monthly averages for total concentrations (mg/L) of oil and grease in produced water for ocean disposal permitted by different countries [99]. .	35
Table 1.5 US EPA 16 priority-pollutant PAHs.....	37
Table 1.6 Target molecules focused on in this work	41
Table 2.1 HSP values of solvents and swelling factor for PMMA	46
Table 2.2 Calculated RED and R_a values for solvents used in the swelling tests.....	48
Table 2.4 RED value and HSPs of mixed solvents.....	57
Table 3.1 GC-MS mode parameters used to identify the PAHs	67

List of Symbols, Nomenclature or Abbreviations

AED	Atomic emission detector
AIBN	Azobisisobutyronitrile
BTEX	Benzene, Toluene, Ethylbenzene and Xylenes
C-NLOPB	Canada-Newfoundland and Labrador Offshore Petroleum Board
C-NSOPB	Canada-Nova Scotia Offshore Petroleum Board
DME	Dimethoxyethane
DCM	Dichloromethane
DMPA	2, 2-Dimethoxy-2-phenylacetophenone
EI	Electron ionization
EGDMA	Ethylene Glycol Dimethacrylate
ECD	Electron capture detector
FID	Flame ionization detector
FPD	Flame photometric GC-MS detector
GC-MS	Gas chromatography- mass spectrometry
HSP	Hansen Solubility Parameter

HPLC	High performance liquid chromatography
IF	Impact factor
KPS	Potassium persulfate
LC	Liquid chromatography
MAA	Methacrylic acid
MIP	Molecularly imprinted polymers
MPa	Mega Pascal
MSD	Specific detectors include
NAB	National Energy Board
NIP	Non-imprinted polymer
NIST	National Institute of Standards and Technology
NPD	Nitrogen-phosphorus detector
PAH	Polycyclic aromatic hydrocarbons
PC	Polycarbonate
PE	Polyethylene
PID	Photoionization detector
PLC	Poly-(caprolactone)

PET	Poly-(ethylene terephthalate)
PEGMM300	Poly-(ethylene glycol) average Mn 300
PMAA	Poly-(methacrylic acid)
PTHF	Poly-(tetrahydrofuran)
R_0	Interaction radius
R_a	Solubility distance
RED	Relative energy distance
SCD	Sulfur chemiluminescence detector
SEM	Scanning electron microscopy
SIM	Selected ion monitoring
TCD	Thermal conductivity detector
TEA	Thermal energy analyzer
UV	Ultraviolet
US-EPA	United States Environmental Protection Agency
δ_d	Cohesive energy from dispersion forces
δ_p	Cohesive energy from polar–polar forces
δ_h	Cohesive energy from hydrogen bonding forces

List of Appendices

Appendix A..... 96

Appendix B..... 99

Chapter 1. Introduction and Literature Review

1.1 Introduction to synthesis of porous polymers

1.1.1 Macroporous copolymer networks

Macroporous copolymer networks are a class of materials featuring permanent porosity with pore sizes between 50 and 200 nm [1]. Applications for macroporous polymers that depend on specific properties, the parameters that can be tuned to yield necessary features need to be understood and characterized [2,3]. These properties include but are not limited to pore size, specific surface area, porosity, particle diameter, and particle shape [4, 5]. The applications of macroporous polymers are profuse, for example, ion exchange resins [3], sorbents for chromatographic separations or sample preparation [6], as catalyst supports [7], and biomedical applications (*e.g.*, *in vivo* time-release of pharmaceuticals) [8].

The first porous polymers were synthesized in the 1930s by free-radical copolymerization of styrene and divinylbenzene; this was followed by solvent mediated pore-swelling to impart porosity. Since the pore structures of the polymers resulted from swelling in the solvent, the polymers had negligible inherent porosity which restricted their utility [9]. Toward the end of the 1950s, a new polymerization method was developed that yielded polymers with permanent porous structures; details of this work were reported more recently by Okay [3]. This method involved suspension polymerization of divinylbenzene and styrene in a solvent that would solubilize the prepolymerization mixture

(monomers, cross-linkers and initiator), but did not dissolve the resulting copolymeric networks, thereby leaving behind a porous structure. By virtue of their porosity and the size of the pores created, these copolymeric networks were characterized as macroporous polymers [3].

Over the past 50 years, synthesis and development of macroporous polymer networks of different chemical compositions have been used in many studies to produce polymeric materials in different formats (*e.g.* monoliths and particles). Monoliths can be used intact or broken up mechanically to particles of a desired size. Particulate materials can be prepared using various approaches, such as microemulsions and precipitation polymerization. Recent examples of new macroporous polymers include the development of monoliths for high performance liquid chromatography [10], capillary electrophoretic chromatography [11], microfluidic reversed phase chromatography [12], nano-liquid chromatography [13], separation of proteins [8], as well as the microfluidic synthesis of macroporous copolymers particles with extremely narrow size distribution [14]. When used as a chromatographic packing material, particulate polymeric materials can suffer from high initial flow resistance and breakthrough. As an alternative, monoliths have exhibited excellent performance characteristics when compared to particulate polymers, particularly with high eluent flow rates and when rapid mass transfer and equilibration are necessary.

Polymeric coatings can be monolayers, ultra-thin (10s of nm) or thicker. Above a monolayer, coatings are accurately described as monolithic polymer coatings; these take advantage of the simple fabrication associated with monolith production to make a surface

that can be used in a range of analytical applications. To be suitable for analytical purposes, an ideal monolithic coating would allow for fast equilibration between adsorbent and target analyte; this requires that polymer have high surface area with well controlled mesoporous structures. There are several methods for making rigid macroporous monolith polymers [15, 16].

1.1.2 Techniques for fabrication of macroporous particulate polymers and monoliths

Polymeric particulate packings have traditionally been obtained from bulk monoliths that are ground and sieved to isolate the correctly-sized particles; the approach is inherently wasteful [17]. Polymeric particulate porous microspheres can be produced more efficiently by suspension polymerization [18]. The porogen is usually miscible with the prepolymerization mixture but is immiscible with the copolymeric network. The polymerization reaction takes place in the presence of cross-linker molecules. During polymerization, the presence of the solvent leaves behind the porous polymeric networks formed during phase separation [19, 20]. Another strategic fabrication method relies on injection of a prepolymerization mixture (monomer, an initiator, and a solvent) into a phase in which it is immiscible thereby forming droplets. The formation of macroporous polymer particles by polymerization and swelling technique is illustrated in Figure 1.1 [21]. In this technique, polystyrene particles can be used as seed particles. The particles were swollen with butyl phthalate, which is also the activator. Next, the swollen template particles are treated with a mixture of monomer, porogen, and free-radical initiator, which increases the

degree of swelling and pore volume. Formation of copolymeric network and removal of the immiscible solvent results in macroporous particles with a mean diameter of 7-8 μm .

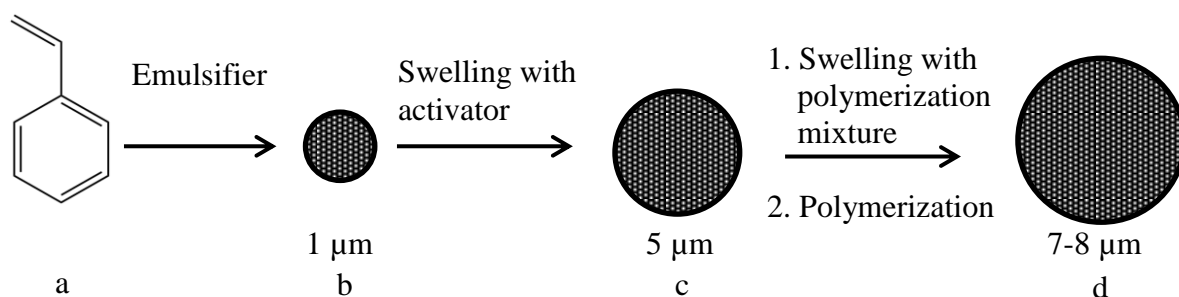


Figure 1.1 Preparation of porous beads using the swelling and polymerization technique. Copyright 1992 Wiley-VCH[21]. a) Styrene (monomer), b) monodisperse particulate template, c) swollen template particles, d) porous beads.

Monolithic coatings are typically prepared in a tailored format by a molding process (Figure 1.2) using a rigid mold. In this process, the mold is filled with prepolymerization mixture containing a monomer, cross-linker, polymerization initiator, and porogenic solvent. Polymerization is initiated by exposure to UV light or via heating at temperatures ranging between 55–80 $^{\circ}\text{C}$ [15, 22]. In contrast to suspension polymerization that yields polymers with a large irregular and very large pore structure, this process yields porous structure monoliths with unique porosity containing large micron-sized pores coexisting with smaller, *ca.* 10 nm, size pores. [16].

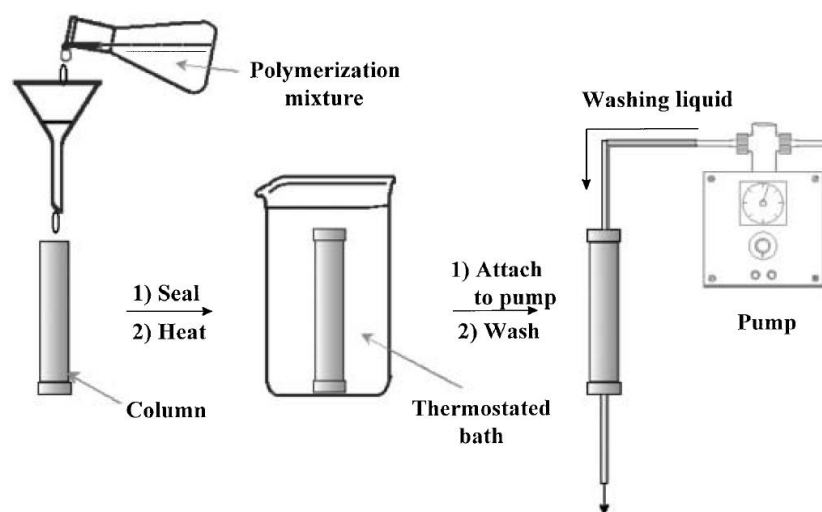


Figure 1.2 Example of preparation of macroporous polymer monoliths [23]. Copyright © 2002, Springer-Verlag Berlin Heidelberg.

1.1.3 Formation of polymers with porous structures

Free-radical cross-linking copolymerization for synthesis of macroporous copolymers, mentioned previously in this chapter, usually involves a photo or thermal initiator along with a vinyl monomer, a divinyl cross-linker, and the solvent (porogen). Free-radicals are created by decomposition of the initiator, which induces the polymerization and cross-linking reactions to form a three-dimensional polymeric network starts to form. The point at which the system has transformed from the liquid to the solid phase is called the “gel point”. Phase separation is said to occur when the growing polymer is no longer solubilized by the solvent (porogen). At this point, the growing polymer becomes insoluble and phase separation occurs to yield a solid or gel-like polymer. The better the solvent is at solubilizing the growing polymer, the later phase separation will occur. When monomer

and cross-linker remaining in solution, the polymer can continue to grow, building on the scaffold that is formed when phase separation is achieved. As the polymer grows, porosity and performance characteristics can change, making the optimization of fabrication challenging. For example, polymers fabricated by free-radical cross-linking copolymerization may have different porous structures depending on the nature and amounts of the monomer, cross-linker, and porogen used in the reaction. Particularly important is the solvation power of the porogen for the given polymer components [3].

Generally, a solvent that is thermodynamically-compatible with copolymeric network is called a “good” solvent. In contrast, a solvent with poor thermodynamic-compatibility with the copolymeric network is called a “bad” or poor solvent. Using a poor solvent as the porogen causes early phase separation during the reaction. This phase separation may occur before the gel point. Early phase separation results in the formation of a discontinuous polymer phase in a continuous phase containing monomer, cross-linker and porogen. After polymerization, the aggregated cross-linked particles further aggregate into larger clusters. This results in an increased pore volume and formation of larger pores and lower polymer surface area. On the other hand, if a *good* solvent is used, then phase separation occurs at a much later stage of the polymerization. After the onset of the polymerization and cross-linking process, nuclei are continuously generated and react with each other. The agglomeration processes result in the formation of a heterogeneous gel. After removal of the porogen from the gel, polymers with small pores and large surface area are formed [24-27].

The solubility of the polymer in the porogen has a crucial effect on the porosity of the macroporous polymer [28, 29]. Table 1.1 shows that the morphology of macroporous polystyrene-divinylbenzene varies depending on the choice of porogen. According to Table 1.1, poor solvents facilitate the formation of large clusters and hence larger pores. Therefore, macroporous polystyrene-divinylbenzene polymers with a low surface area (up to 100 m²/g) can be synthesized. In contrast, by increasing the solvation power of the porogen (i.e., by using a *good* solvent), the number of micropores and surface area increase, and the average pore diameter significantly decreases [3].

Table 1.1 Controlling morphology of styrene-divinylbenzene by changing the solvation power of the porogen [30]

Pores characteristics	Good Solvent (e.g., toluene, dichloroethane)	Poor Solvent (e.g., n-heptane, alcohols)
Mean pore diameter	Small	Large
Specific surface area [m ² /g]	50-500	10-100
Pore volume [mL/g]	< 0.8	0.6-2.0
Pore wall surface	Smooth surface	Irregular rough surface
Pore size distribution	Predominantly microporous (20 Å) and mesoporous (20-500 Å)	Predominantly mesoporous (20-500 Å) and macroporous (over 500 Å)

The solvation power of the porogen can be measured by the difference between the solubility parameters of the porogen, δ_1 , and the copolymer, δ_2 [3, 28, 31]. According to Dušek *et al.* [32], the porous structure formation mainly depends on the phase separation step, which is caused by the change in the interaction between polymer and porogen. Through the use of solubility parameters, the compatibility of the porogen with the polymer components with respect to phase separation behaviour can be studied systematically, which should make it possible to develop a more efficient approach to fabrication of porous polymers with desired characteristics.

1.2 Solubility parameters

Solubility parameters have been used extensively in coating industry to select solvents for coatings materials [33]. Over the past few years, calculation of solubility parameters by computational methods has resulted in successful strategies to optimize the selection of solvent systems for various properties. For example, in response to health and safety or cost saving needs, it might be necessary to replace a solvent in an existing process; by having a more sophisticated algorithm to understand how solvents function, new solvents can be selected to meet a range of criteria while still being fit for purpose [34]. Today most commercial suppliers of solvents widely apply computer programs for solvent selection [35]. Solubility parameters, such as Hansen and Hildebrand solubility parameters, can help to better predict the potential of a porogenic solvent to yield a porous polymer

[36]. They can also be used to predict whether a solvent can dissolve a particular non-crosslinked polymer [37].

1.2.1 Solvation process and the Hildebrand solubility parameters

Thermodynamically spontaneous solvation processes require that the change in the Gibbs energy of the process be zero or negative. The Gibbs energy change for the solvation process can be broken into enthalpic and entropic components as follows:

$$\Delta G_M = \Delta H_M - T\Delta S_M \quad (1.1)$$

ΔG_M is the Gibbs energy of mixing, ΔH_M is the enthalpy of mixing, T is the temperature, and ΔS_M is the entropy of mixing. Hildebrand and Scott [38] proposed that the enthalpy of mixing could be measured by:

$$\Delta H_M = V_{mix} \left[\left(\frac{\Delta E_1^V}{V_1} \right)^{\frac{1}{2}} - \left(\frac{\Delta E_2^V}{V_2} \right)^{\frac{1}{2}} \right]^2 \varphi_1 \varphi_2 \quad (1.2)$$

Where V_{mix} is the volume of the mixture, ΔE_i^V is the vaporization energy of the species i (for example the solvent and the polymer), V_i is the molar volume of species i , and φ_i is the volume fraction of the species. The cohesive energy (E_{coh}) is related to the intermolecular forces that are present in a system and are typically expressed as the difference in internal energy per mole (which can be expressed as a volume for a pure substance, V_m) for a substance when there are intermolecular forces at play to the internal energy when

there are none. This relationship can be expressed as follows:, where e_{coh} is the cohesive energy density given in J cm⁻³ or MPa [39]:

$$e_{coh} = \frac{E_{coh}}{V_m} \quad (1.3)$$

From Equation 1.3, the Hildebrand solubility parameter (δ) was derived as the square root of the cohesive energy density to yield Equation 1.4 [39-41].

$$\delta = \left(\frac{E_{coh}}{V_m} \right)^{\frac{1}{2}} = e_{coh}^{\frac{1}{2}} \quad (1.4)$$

Equation 1.2 can be written in terms of the Hildebrand solubility parameter:

$$\frac{\Delta H_M}{V} = \varphi_1 \varphi_2 (\delta_1 - \delta_2)^2 \quad (1.5)$$

The enthalpy of mixing determined by Eq 1.5, must be smaller than the entropic term (in Eq 1.1) to satisfy the $\Delta G_M \leq 0$ requirement. Therefore, the solubility parameters difference ($\delta_1 - \delta_2$) needs to remain small.

Hildebrand parameters have been used by industry to the prediction of the permeation rate, mechanical properties, and chemical resistance of polymers [40]. They also have many applications in the study and control of solvent-polymer behavior. This includes control over the pore size distribution during synthesis, and suitability for dissolution, suspension, or swelling of the polymer within the solvent. Goh *et al.* [42] have studied the effect of solubility parameters of solvents on the morphology of cross-linked

poly(methacrylic acid-*co*-poly(ethylene oxide) methyl ether methacrylate) polymers prepared by suspension polymerization. It was observed that ketone and ester solvents caused rough but colloidally stable microspheres. Alcohols and hydrocarbons resulted in soluble polymers and aggregated particles, respectively. Since the Hildebrand solubility parameters correspond to the cohesive energy of solvents and polymers, they can be used to rationalize the polymer morphology observed in the presence of different solvents. For example, the Hildebrand solubility parameter of a mixture of 80% toluene and 20% DME by volume is $18 \text{ MPa}^{1/2}$. Polymerization in this solvent resulted in irregular agglomerated particles, whereas polymerization from a solvent like ethyl acetate ($18.2 \text{ MPa}^{1/2}$) resulted in microspheres. The main disadvantage of the Hildebrand parameter is that it does not consider specific interactions between molecules (*e.g.*, dipole-dipole interactions). Consequently, a more nuanced approach has been taken in the development of alternative models. Thus, the three-dimensional Hansen solubility parameters (HSP) are more practical than the isotropic Hildebrand parameter in terms of understanding the role of the solvent in the polymerization system

1.2.2 Hildebrand and Hansen solubility parameters

The Hildebrand solubility parameters are used as an indicator for the affinity of the polymer for the solvent, however, Charles M. Hansen attempted to divide the overall interactions between a solvent and a solute into polar, dispersive, and hydrogen-bonding interactions [34, 43]. The theory behind the HSP is described in his thesis (1967), which is still relevant today [34].

Hansen expressed the three types of interactions in the following way [34].

$$E = E_D + E_P + E_H \quad (1.6)$$

The total cohesive energy (E) is the sum of the energy from dispersion (D), dipole-dipole (P), and hydrogen bonding (H) forces between molecules. Dividing Eq. 1.6 by the molar volume gives the square of the total Hansen solubility parameter as the sum of the squares of the Hansen δ_d , δ_p and δ_h [44].

$$\frac{E}{V} = \left(\frac{E_D}{V}\right) + \left(\frac{E_P}{V}\right) + \left(\frac{E_H}{V}\right) \quad (1.7)$$

$$\delta^2 = \delta_D^2 + \delta_P^2 + \delta_H^2 \quad (1.8)$$

1.2.4 Three-dimensional Hansen space

In the three-dimensional Hansen space δ_d , δ_p and δ_h are three perpendicular axes which are plotted in the Hansen sphere. The center of the Hansen sphere incorporates the δ_d , δ_p , and δ_h of the polymer, which is shown by points and has a constant value. Each solvent (including solvent mixtures) is also represented by a point in Hansen space. Thermodynamically-compatible solvents are inside the sphere, while thermodynamically-incompatible solvents are excluded from the Hansen sphere. There are also boundary conditions at the surfaces of the Hansen sphere, the radius of the Hansen sphere (see below), which is where the polymer or solute undergoes phase separation from the solvent;

for example, the conditions for solvation are no longer met [34]. Figure 1.3 illustrates the three-dimensional Hansen sphere.

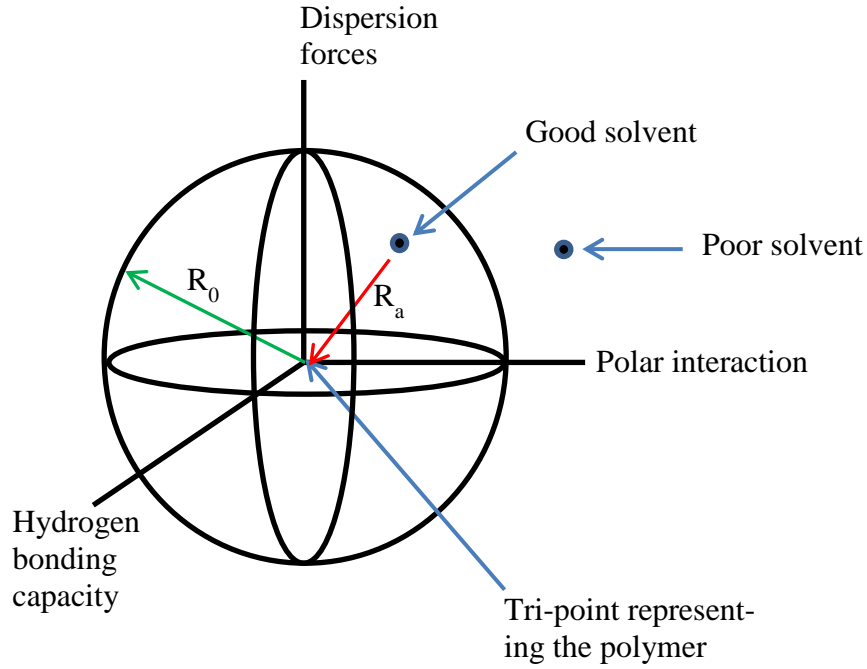


Figure 1.3 Three-dimensional Hansen space.

The radius of the Hansen sphere is also described as the radius of interaction (R_0). Solubility distance (R_a), which can be calculated for any polymer-solvent combination, shows the distance between solvent and solute in Hansen space. Once the polymer HSPs are determined, the distances between solvents HSP and a polymers HSP in Hansen space can be calculated by Equation 1.9:

$$R_a = \sqrt{4(\delta_{D2} - \delta_{D1})^2 + (\delta_{P2} - \delta_{P1})^2 + (\delta_{H2} - \delta_{H1})^2} \quad (1.9)$$

Dividing the solubility distance, R_a , by the interaction radius R_0 (determined through Hansen algorithm) yields the “relative energy distance” (RED), which shows the compatibility of the solvent and polymer.

$$RED = \frac{R_a}{R_0} \quad (1.10)$$

If the RED is 0, then there is no energy difference between solvent and solute/polymer ($R_a = 0$) and the polymer is soluble. Practically, if the solubility parameters are closely matched, then the RED will be less than 1 and the solvent and solute are strongly compatible and predicted to be soluble. When the RED is close to 1, then the system is near the boundary condition. If the RED value is higher than 1, then lower affinities of solvent for solute are indicated [34, 43]. The consequences of these values will be discussed later in greater detail.

1.2.5 HSP determination of polymers

The porosity of highly cross-linked insoluble polymers can also be predicted and controlled by the HSP theory. One method to calculate the HSPs and interaction radii of insoluble polymers is based on swelling tests with different solvents. This data can be used to calculate the HSPs of a polymer. This method of determining the HSPs of a polymer is much more effective than other methods that depend on correlation with intrinsic viscosities or pure statistical analysis [2]. The HSPs of most polymers are determined by experimental procedures followed by theoretical models, or group contribution techniques,

which have been optimized by regression and fitting methods [45, 46]. The HSPs of polymers are usually calculated by testing the degree of interaction with a large variety of solvents through swelling experiments to obtain swelling factors and applying the Hansen algorithms to correlate experimental data with solvent HSPs [34]. The HSPs of a large range of common solvents have been calculated and reported in the literature [1, 34, 47]. However, only a small number of polymers have known Hansen solubility parameters [2, 46]. Table 1.2 describes HSPs of some common solvents.

Table 1.2 HSPs of some common solvents [34].

Solvent	δ_d	δ_p	δ_h	Solvent	δ_d	δ_p	δ_h
Benzene	18.4	0.0	2.0	n-Butyl acetate	15.8	3.7	6.3
Toluene	18.0	1.4	2.0	sec-Butyl acetate	15.0	3.7	7.6
Xylene	17.6	1.0	3.1	Dimethyl phthalate	18.6	10.8	4.9
Ethyl benzene	17.8	0.6	1.4	1,4-Dioxane	19.0	1.8	7.4
Styrene	18.6	1.0	4.1	Chloroform	17.8	3.1	5.7
Decalin (cis)	18.0	0.0	0.0	Chlorobenzene	19.0	4.3	2.0
Tetralin	19.6	2.0	2.9	Carbon Tetrachloride	17.8	0.0	0.6
Cyclohexane	16.8	0.0	0.2	Methylene dichloride	18.2	6.3	6.1
Methyl cyclohexane	16.0	0.0	1.0	Methanol	15.1	12.3	22.3
n-Pentane	15.6	0.0	0.0	Ethanol	15.8	8.8	19.4

n-Hexane	14.9	0.0	0.0	n-Propanol	16.0	6.8	17.4
n-Heptane	15.3	0.0	0.0	Ethylene carbonate	19.4	21.7	5.1
n-Octane	15.5	0.0	0.0	γ -Butyrolactone	19.0	16.6	7.4
n-Nonane	15.7	0.0	0.0	N,N-dimethyl formamide	17.4	13.7	11.3
Acetone	15.5	10.4	7.0	N,N-dimethyl acetamide	16.8	11.5	10.2
Methyl ethyl ketone	16.0	9.0	5.1	Dimethyl sulfoxide	18.4	16.4	10.2
Methyl isobutyl ketone	15.3	6.1	4.1	Tetramethylene sulfoxide	18.2	11.0	9.1
Cyclohexanone	17.8	6.3	5.1	Water	15.5	16.0	42.3
Ethyl acetate	15.8	5.3	7.2				

1.2.6 The general Hansen algorithm

Figure 1.4 depicts a flowchart of the Hansen algorithm used in this thesis to determine the HSPs for a model polymer system. The input data contains a list of n solvents ($n = 1, 2, \dots$) that were used for swelling test with their known HSPs (δ_{di} , δ_{pi} , δ_{hi}) as well as swelling factors ($S_i = 0, 1$) [2]. The swelling factor is a binary assessment of the interaction between polymer and solvent. No swelling of the polymer in the solvent results in a swelling factor equal to 0. In contrast, the swelling factor is 1 when a polymer shows any evidence of swelling in the solvent [34]. Swelling is estimated by mass change in the polymer. Using the binary data and HSP data for the solvents, the program can be used to determine HSP values for a given polymer system. The iterative calculations start with an

initial calculation of a set of HSPs and interaction radius for the polymer (δ_{di} , δ_{pi} , δ_{hi} , and R_0). For each set of calculated HSPs and interaction radius, the quality-of-fit function is used to evaluate the input data is for swelling. The quality-of-fit function is a desirability function, but in Hansen's work, the quality-of-fit function is designated as the *DATAFIT* function, which takes the following form:

$$DATAFIT = \sqrt[n]{(A_1 \times A_2 \times \dots \times A_n)} \quad (1.11)$$

where n is the number of solvents and the A_i has the form:

$$A_i = e^{-[ERROR\ DISTANCE\ (i)]} \quad (1.12)$$

ERROR DISTANCE (i) is the error in the differences of R_a and R_0 . The ERROR DISTANCE is 0 and A_i quotient is 1 when a solvent is inside the sphere (a good solvent) with $S_i = 1$ and $R_{ai} < R_0$. A poor solvent will yield $R_{ai} > R_0$ outside the sphere with the $S_i = 0$. If a *good* solvent ($S_i = 1$) is outside the sphere ($R_{ai} > R_0$), then the A_i quotient is calculated by:

$$A_i = e^{-(R_{ai}-R_0)} \quad (1.13)$$

If a poor solvent ($S_i = 0$) is inside the sphere ($R_{ai} < R_0$), then the A_i quotient is calculated by:

$$A_i = e^{-(R_0-R_{ai})} \quad (1.14)$$

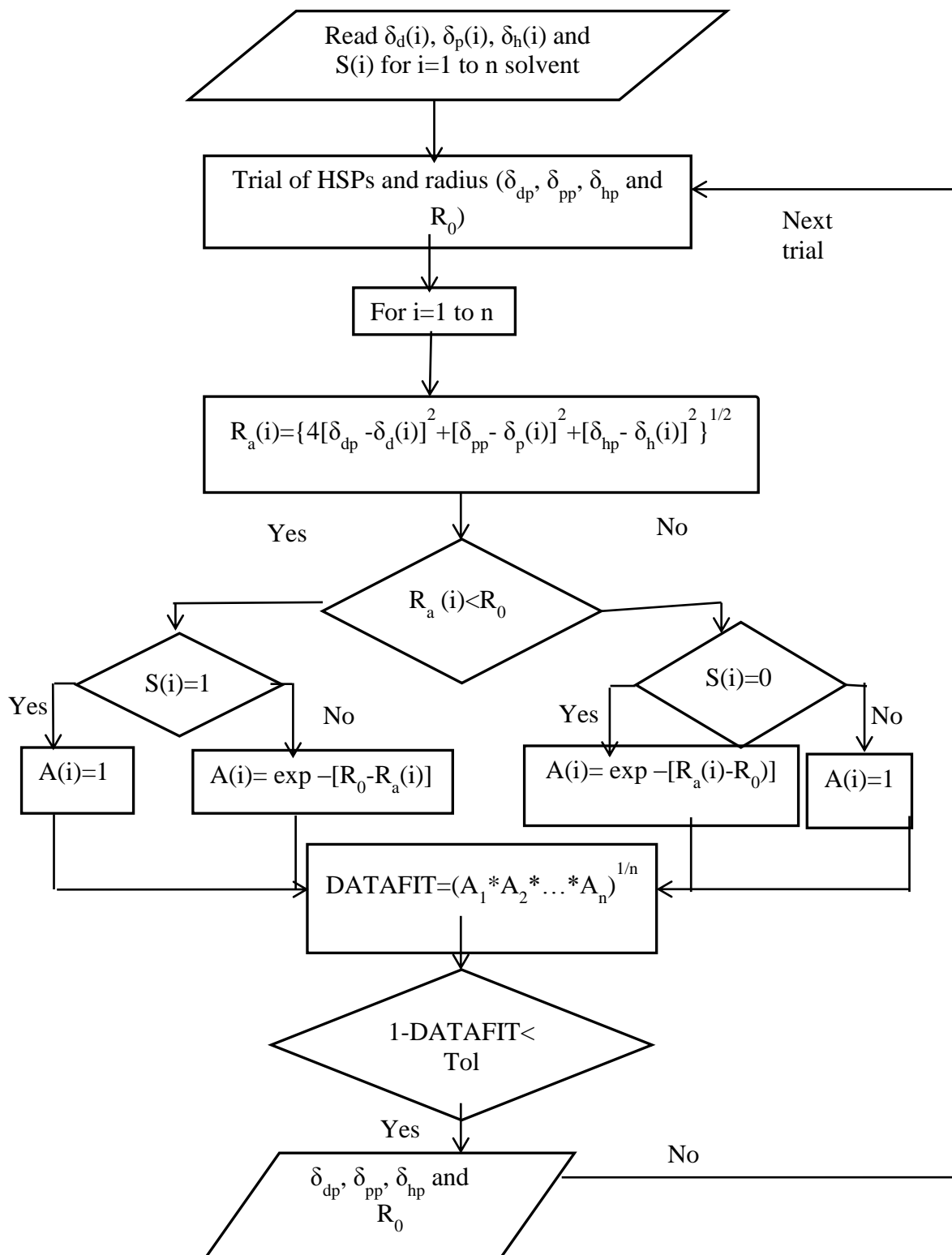


Figure 1.4 General flowchart of Hansen algorithm[2].

Therefore, A_i quotients always are between 0 and 1, which makes the DATAFIT function limited to the same range (according to Eq. 1.11). Improvement of fitting during optimization results in a DATAFIT that approaches 1. To achieve a DATAFIT equal to 1, all good solvents must be inside the sphere and all the poor solvents must be outside the sphere.

1.2.7 Selection of pore-former solvent based on HSPs

HSPs are practical criteria that allows the thermodynamic compatibility of a porogen with a polymeric network to be predicted. One can determine whether a porogenic solvent can give a rough polymer with good porosity by comparing the positions of the solvent with respect to its polymer-solubility in three-dimensional Hansen space [34].

As the polymerization process proceeds, the polymeric network forms due to the relative difference in HSP between the copolymer and the porogen ($|\Delta\delta|$). Those porogens that are outside the Hansen sphere have large $|\Delta\delta|$ values and $RED > 1$, which make these porogens poor solvents. These solvents cause early phase separation and yield polymers with large pore structures (macroporous) and low surface areas. On the other hand, $|\Delta\delta|$ value is small for *good* solvents that exist inside the Hansen sphere with $RED < 1$. These solvents cause late stage phase separation and a unimodal microporous resin with high surface area. In addition, solvents which are inside the sphere can dissolve or swell the polymeric network. Solvent systems that are on the boundary with moderate $|\Delta\delta|$ values and REDs equal to, or close to, 1 show a balance between the advantages of the microporous gels, which have high surface area but slow mass transport, and fully

macroporous structures with low surface area. Such moderately good porogens give polymers with excellent porosity and ideal morphology for the molecularly imprinted polymer films targeted in our group [20, 43].

1.3 Molecularly imprinted polymers (MIPs)

Molecular imprinting is a technique based on polymerization in the presence of a template molecule. The template molecule is selected such that the polymer will exhibit selective recognition of target molecules in various matrices [48]. Molecularly imprinted polymers (MIPs) are tunable macromolecules containing cavities that are complementary in shape and size to template molecules present during polymerization. These unique features enable MIPs to bind selectively to target analytes that have similar shape and size to the template molecule [49].

In comparison to many other molecular recognition materials, MIPs are relatively easy to make, robust, and inexpensive. Given this, MIPs have been featured in a variety of applications in many fields such as sensor technology (chemo- and bio-sensors) [50], chromatographic columns [51], enzyme catalysts [52], water purification [53], and artificial antibodies [54]. MIPs have been prepared using various polymerization methods including precipitation [55], emulsion [56], and suspension polymerization grafting methods [57]. Bulk polymerization to form monoliths frequently require further processing, like grinding and sieving, for analytical applications [58, 59]. The resulting particles show irregular sizes and shapes. Moreover, grinding degrades the quality of the polymer leading to loss of selective binding sites [60]. Alternatively, MIPs can be made as thin films on an inert

surface such as a microscopic glass slide. Thin film technique can provide homogeneous MIPs with desired surface area and binding sites for detecting targets [61, 62].

1.3.1 Molecular imprinting strategy

MIPs are generally synthesized through the following steps (Figure 1.5). (1) Formation of a pre-polymerization complex using monomer and template through self-assembly interactions. In this step, the functional monomers interact with template to create specific recognition sites. (2) Polymerization of the pre-formed complexes with cross-linker molecules to form a rigid polymeric matrix. This step is usually activated by a polymerization initiator. (3) Extraction of the template molecules leaving behind the binding sites with specific recognition properties for target molecules, which are capable of selectively binding to the structural analogous target molecules [55, 63, 64].

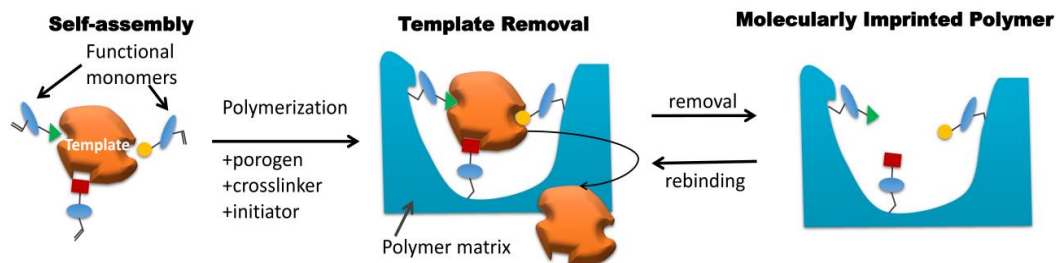


Figure 1.5 Molecularly imprinted polymer fabrication.

1.3.2 Factors affecting molecular recognition in MIPs

Although the fabrication of MIPs is simple, to achieve a high level of molecular recognition, one requires a good understanding of polymer chemistry, molecular recognition theory, chemical equilibria, and thermodynamics [65]. For example, MIPs need to be sufficiently rigid to maintain the structure of the cavities after the templates removal. On the other hand, the polymers should be flexible enough to release the template through swelling and extraction, and subsequently return to the ideal morphology for uptake of the target molecules. These two parameters may be contradictory to each other. Therefore, an attentive optimization is necessary for making MIPs [66]. Fabrication of MIPs can be challenging due to a large number of elements involved, *e.g.*, the selection of template, functional monomer, cross-linker, porogen, and initiator [67].

(a) Template

The role of the template molecule is to organize the functional group of monomers during the molecular imprinting processes [68]. Template imprinting occurs during the polymerization process. After the polymerization, the template molecules are removed from the polymeric network. Template removal produces cavities or recognition sites that are similar to the template molecules in terms of size, shape, and functionality. The template must be stable during polymerization. For example, in free-radical polymerization, the template should be chemically inert to avoid participation in radical reactions during polymerization [69]. Template extraction is a critical step in the preparation of MIPs. In an ideal system, the template molecule would be the molecule that one intends to target in

their applications. However, even when template removal is highly efficient, traces of the template remaining in the MIP can lead to false positive detection. To avoid this problem, pseudo-templates can be used for imprinting [61]. A pseudo-template is a molecule that is similar to the target molecule in terms of shape, size, and key functional group orientation, but can be easily distinguished from the target at the time of analysis. The ideal pseudo-templates are isotopically labelled analogues, which one could argue are indistinguishable from the target except by mass spectrometry. However, these are expensive and are only suitable for detection by mass spectrometry, so structurally similar molecules can be good options for imprinting. However, in such cases, selection of the best pseudo-template is not trivial.

(b) Functional monomer

A functional monomer must interact with the template molecule; this can occur through a range of bonding types, including covalent and non-covalent (*e.g.* hydrogen bonding) through. The stoichiometry between the monomers and template will depend on the number of functional groups through which bonding can occur and the strength of the interactions; therefore optimization of the stoichiometry can be a challenge [70]. It is critical for the monomer to have functional groups that complement the functionality of the template molecule (*e.g.*, H-bond acceptor and H-bond donor) to ensure an efficient imprinting effect [71]. Figure 1.6 shows a selection of typical functional monomers used for the fabrication of MIPs. Among these monomers, MAA has been widely used as a functional monomer due to its hydrogen bond donor and acceptor properties [63]. According to

Zhang *et al.* [72], MAA has a high degree of desirable functionality relative to its mass, which tends to produce porous polymeric materials with excellent binding capacity.

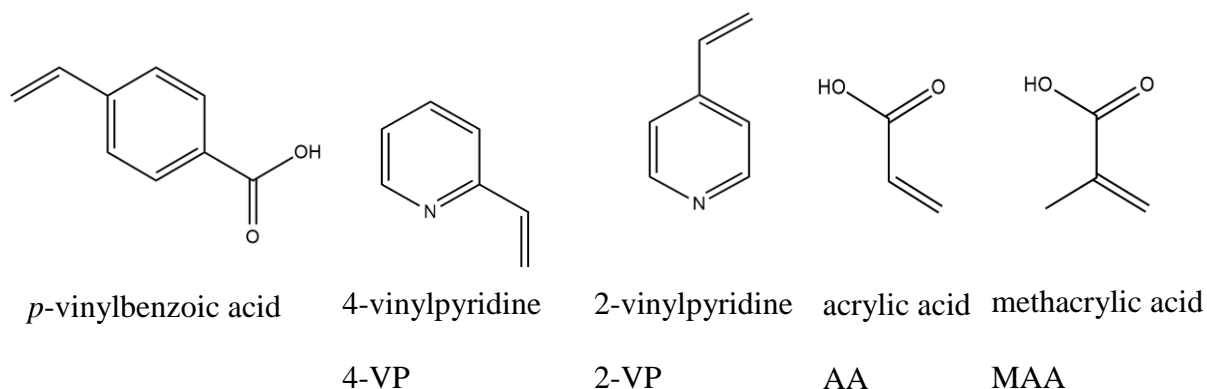


Figure 1.6 Typical functional monomers used for fabrication MIPs.

(c) Cross-linker

The cross-linking agent, or cross-linker, is a multifunctional molecule, typically divinyl, that can copolymerize with the monomer while in a complex with the template form a three-dimensional cross-linked polymeric network around the template. The amount and the type of the cross-linking agent can greatly affect the selectivity of MIPs. In a typical molecular imprinting procedure, the cross-linker it stabilizes the imprinted binding sites, imparts mechanical stability to the polymeric network and is involved in control of polymer morphology [73].

Generally, in the polymerization process, a high loading of cross-linking agent is required to produce polymer with permanent porosity, stable recognition sites, and adequate mechanical stability by forming a more rigid three-dimensional structure. As a result, the functional groups are preserved in an appropriate configuration for binding the target molecules [74]. Ethylene glycol dimethacrylate (EGDMA) is a common cross-linking agent due to its ability to produce a polymer with high binding capacity and selectivity and its compatibility with hydrophilic solvents [66].

(c) Porogen

The porogenic solvent, or porogen, is used to dissolve the pre-polymerization compounds, therefore, the functional monomer, template molecule, cross-linker, and initiator must be soluble in the porogen. Additionally, the porogen should not interfere with the formation of the pre-polymerization complex between the template and the monomer, *e.g.*, water disrupts hydrogen bonding, toluene interrupts π - π interactions [74]. As discussed previously, it is recognized that solvent plays a key role in pore generation, influencing shape, size, and volume of the pores in polymeric systems, including MIPs. [25, 66].

(e) Initiators

An initiator is essential for formation of sufficient free radicals for an efficient radical polymerization process. Normally, an initiator is added in a small amount in comparison with monomer, template, and cross-linker ratios. Based on the chemical properties of the initiator, it decomposes to form radicals by different mechanisms. These routes include,

but are not limited to, UV light, heat, or by other chemical or electrochemical methods [75]. For instance, azobisisobutyronitrile (AIBN) molecule decomposes by heating to give a stable radical carbon center that is efficient in initiating polymerization of vinyl monomers. Figure 1.7 shows the generation of a carbon radical by thermal decomposition of AIBN [76].

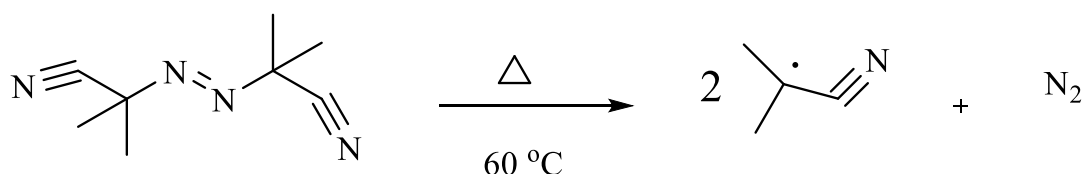


Figure 1.7 Formation of carbon centered radical by thermal decomposition of AIBN.

1.3.3 Molecular imprinting approaches

Generally, two molecularly imprinting approaches have been employed for fabrication of MIPs. One method is based on covalent interactions, while the other more broadly applicable method is based on non-covalent molecular interactions between the functional monomer and the template; these are illustrated in Figure 1.8 [73]. In both cases, the functional monomer interacts with the template to form a stable pre-polymerization complex.

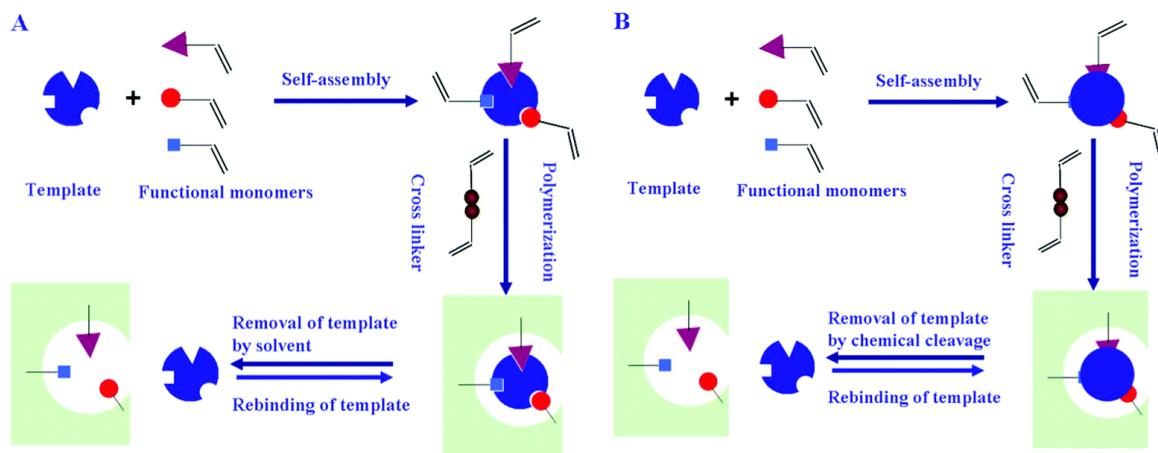


Figure 1.8 Non-covalent and covalent molecular imprinting approaches. Used with permission [77].

In fully covalent molecular imprinting, which was proposed by Wulff [78], the template molecule is covalently bound to the functional monomer. Analyte re-binding in this method requires that the covalent bond can be cleaved to remove the template and that it can be reformed for uptake of the analyte. [79]. The covalent imprinting approach yields very stable and selective MIPs. These interactions can also result in more homogeneous binding sites than the non-covalent methods due to the explicit control of the stoichiometry between the template and the monomer. However, covalent imprinting has its weaknesses. For example, there are a limited number of functional monomers that can undergo rapid reversible covalently reactions with a large range of candidate template molecules. Also rebinding of the templates is difficult because of the challenges associated with re-forming the covalent bonds, particularly in aqueous environments [80].

Non-covalent molecular imprinting, pioneered by Mosbach and co-workers in the mid-1980s [81], is more widely used than the covalent approach because of its simplicity and adaptability. It relies on spontaneous self-assembly through weaker interactions, such as van der Waals forces, π - π interactions, and hydrogen bonding. This is analogous to molecular recognition in living system, such as when enzymes and antibodies recognize their target molecules through hydrogen-bonding, electrostatic interactions and hydrophobic interactions [82, 83]. Though less specific or permanent than covalent imprinting, template-monomer complexation can occur through a range of common interactions. The combination of interactions makes it easier to find monomers for a given template. The geometry established in the self-assembly process is fixed through polymerization, usually with a high degree of cross-linking [84]. Both template removal and reuptake are easier in non-covalent imprinting. It is much easier to disrupt weak bonding interactions under mild conditions to remove the template and reuptake of the target analyte is generally straightforward in a range of media without the need for reagents to reform covalent bonds [63].

A disadvantage of non-covalent imprinting is that the interactions between template and functional monomer are not strong. Since the interactions are controlled by an equilibrium process, the functional monomer needs to be used in excess to move the equilibrium toward the formation of the pre-polymerization complex. This can reduce the selectivity of the material and reduce the efficiency of the rebinding process [80].

Whitcombe *et al.* introduced a semi-covalent method, in which a sacrificial spacer bound the template to the monomer covalently. The spacer was sacrificed in the template re-

moval process. Analyte rebinding occurred through non-covalent interactions [85]. This method takes advantage of the precise stoichiometry and site homogeneity of covalent imprinting with the ease of reuptake associated with non-covalent imprinting.

1.4 Detection methods used with MIPs

1.4.1 Gas chromatography (GC)

GC is used to separate mixtures of compounds, primarily on the basis of boiling point. A GC will consist of an injector, chromatographic column, detector, and data acquisition system. Each section plays an important role in the analysis quality and results [86]. For example, the injector should transfer all compounds in the mixture of analytes to the chromatographic column, without chemical alteration and bias on volatility or molecular weights. Samples are typically volatilized by exposure to the high temperatures in the injection port (200-300 °C) and moved to and through the chromatographic column by a gaseous mobile phase or carrier gas (*e.g.*, He, Ar, N₂ or H₂). The ability of the chromatographic column to separate analytes with very close distribution constants between the mobile and stationary phases is a key advantage GC.

Chromatographic resolution depends on the temperature, stationary phase, mobile phase, and for columns, the size, length, inner diameter, and thickness of the stationary phase. Although columns can be packed or capillary columns, most GC methods used narrow fused-silica capillaries coated on the outside with polyimide. The capillary becomes a chromatographic column when it is coated on the inside with a stationary phase (usually a

hydrocarbon-based coating chemically bound to the silica surface). The chemistry of the stationary phase, in conjunction with the boiling point, allows analytes to be separated and thus reaching the detector at different times (retention time, t_r). Retention (time from injection to detection) of analytes can be used for identification of compounds in the sample mixture [87]. For a complex mixture of analytes with similar structures, a longer column with smaller inner diameter columns is required for a complete compound separation. For instance, the GC analysis of PAHs is usually accomplished using columns that are 30 m long, but the separation of hydrocarbons in gasoline, which is more complex, needs longer columns measuring 100 m [88]. Capillary columns can be classified based on their lengths: short columns (5-15 m), medium columns (20-30 m) and large columns (50-100 m). The most useful column for many compounds, such as pesticides, drugs and PAHs, *etc.*, is the medium capillary column with $L = 30$ m [86], which balances separation efficiency with time of analysis.

Detectors used in gas chromatography are classified as universal, selective and specific universal and near universal detectors. Mass selective detectors (MSDs) and thermal conductivity detectors (TCDs) are counted as the universal detectors. Selective detectors include flame photometric GC-MS detector (FPD), electron capture detector (ECD) and nitrogen-phosphorus detector (NPD). Specific detectors include MSD, thermal energy analyzer (TEA) and atomic emission detector (AED). Frequently detector selectivity depends on the presence of certain atoms (*e.g.*, phosphorus) or functional groups (*e.g.*, nitro) in the analyte structures. For example, a photoionization detector (PID) detects organic carbon, a nitrogen-phosphorus detector (NPD) detects nitrogen and phosphorus, a

sulfur chemiluminescence detector (SCD) detects sulfur and an electron capture detector (ECD) detects compounds with electronegative groups. Compounds with a common fragment such as, benzyl or phenyl, can be detected by an MSD operating in the selected ion monitoring (SIM) mode [89]. Detectors are selected for GC based on their linearity and insensitivity/sensitivity to changes in temperature, pressure, gas flow, for their detection limits, sensitivity, limits of quantitation, and also for their robustness and cost [88].

1.4.2 Gas chromatography-mass spectrometry (GC-MS)

An MS coupled to a GC is typically equipped with an electron ionization (EI) source for ion generation. The molecular ions and fragment ions produced in the source are transferred into the mass analyzer by differential pumping and electrostatic lenses where they are separated based on their m/z ratios [90]. Selected ion monitoring, SIM, is a mode of operation of the MS in which only a set of specific ions with m/z values characteristic of the analyte ions are monitored rather than a full range of m/z values scanned. The SIM mode increases selectivity 30-100 times higher than the full scan mode. GC-MS in the SIM mode effectively provides selective detection of compounds in a complex mixture. Although the SIM mode decreases false positives in compound identification, the identities of analytes must also be confirmed by comparison of retention times of standard compounds [86].

1.5 An overview of produced water

1.5.1 Definition and source

Produced water is a byproduct of the production of oil and gas from onshore and offshore platforms. Produced water includes both injected water and reservoir fluids. Injection water is injected into a reservoir to assist in the recovery of oil and gas [91]. Reservoir fluids include, oil, natural gas, particulates, and formation water, which is seawater that is trapped with oil and natural gas in the reservoir between layers of sediments for millions of years. Produced water is treated to remove most of the oil. It is then discharged into the ocean in offshore operations or into receiving ponds, requiring further treatment, for onshore operations. Reservoir fluids can also be discharged through natural seeps or when the reservoir is penetrated during drilling [92].

During the life of a producing field, the volume of produced water can be ten times higher than the volume of extracted oil and gas; this volume tends to increase as the amount of oil and gas decreases. For older wells, it is common to realize 98% of extracted fluids as produced water (i.e., 2% of the fluid is recoverable oil). The volumes of produced water are immense. For example, in the year 1990, 866 million barrels of produced water were collected in the Gulf of Mexico. Produced water discharged from the Hibernia field in Atlantic Canada was 17,000 m³/day in July 2007 and increased to 20,300 m³/day in September 2007 as the reservoirs were depleted [92].

1.5.2 Chemical composition of produced water

Produced water contains formation water and seawater, which is composed of a complex mixture of wide variety of organic acids, petroleum hydrocarbons, and inorganic materials. The specific composition depends on the local geology, geological age of the field, formation conditions and operational lifetime of the reservoir [93]. Common inorganics are salts such as sodium, calcium, magnesium, potassium, sulfate, chloride, bromide, bicarbonate, and iodide, which are also found in seawater. However, the concentrations of these ions are often higher in the produced water than in seawater, which increases their contribution to the toxicity of produced water [94]. Organic acids (Table 1.4) include mono- and di-carboxylic acids of aliphatic compounds such as propanoic, butanoic, oxalic acid, and benzoic acid [92]. Petroleum hydrocarbons are aliphatic and aromatic hydrocarbons, which as components of produced water, have received the most attention due to their toxicity and other environmental impacts [95].

The presence and distribution of hydrocarbons depend on their water solubility. and They can appear as both dissolved and dispersed (suspension as very small droplets) oil in the produced water [96]. Many of the treatment processes for produced water focus on their removal. Hydrocyclones used in the treatment of produced water rely on centrifugal force to separate dispersed oil droplets, but are ineffective for removal of dissolved components including hydrocarbons, organic acids, phenols, and inorganic compounds from produced water. Consequently, treated produced water discharged into the ocean mostly contains light aromatic hydrocarbons with higher water solubility and higher vapor pressure such as benzene, toluene, ethylbenzene, and xylenes, collectively known as BTEX, light

PAHs, and aliphatic hydrocarbons. Since there are no cost-effective water treatment procedures for use on offshore platforms that can 100% effectively treat produced water, treated produced water still contains dispersed oil that contains higher molecular weight and hydrophobic PAHs such as chrysene and benzo[a]pyrene [97]. As Table 1.4 shows, the total concentration of PAHs in produced water typically ranges from 0.040 mg/L to 3 mg/L. Light PAHs, such as naphthalene, fluorene, and their alkyl homologues, are the most common species. Heavy PAHs are typically not reported as they are mainly associated with the dispersed oil phase due to their low water solubility [98].

Table 1.3 Concentration ranges of natural organic chemicals in worldwide produced water [99].

Organic Chemical	Concentration range (mg/L)
Total organic carbon	≤ 0.1 -11,000
Total organic acids	≤ 0.001 -10,000
Total saturated hydrocarbons	17-30
Total BTEX	0.068-578
Total PAHs	0.04-3.0
Total steranes/triterpanes	0.14-0.175
Ketones	1.0-2.0
Total phenols (primarily C ₀ -C ₅ -phenols)	0.4-23

1.5.3 Regulations

Environmental regulatory agencies are responsible for the regulation of the discharge of produced water into the ocean and other receiving waters. These agencies set limits on the concentrations of petroleum (measured as total oil and grease) in the produced water. For example, the Canada-Newfoundland and Labrador Offshore Petroleum Board (C-NLOPB), the Canada-Nova Scotia Offshore Petroleum Board (CNSOPB) and the National Energy Board (NEB) regulate the discharge of produced water for the Atlantic Canada offshore oil and gas industries [100]. Table 1.5 shows examples of regulations issued by different countries on the concentration of total petroleum hydrocarbon in produced water discharge into the ocean [99].

Table 1.4 Daily maximum and monthly averages for total concentrations (mg/L) of oil and grease in produced water for ocean disposal permitted by different countries [99].

Country	Monthly average (mg/L)	Daily maximum (mg/L)
Canada	30	60
USA	20	42
OSPAR (NE Atlantic)	30	-
Mediterranean	40	100
Western Australia	30	50
Nigeria	40	72
Brazil	-	20

1.6 Polycyclic aromatic hydrocarbons (PAHs)

PAHs are a large and important class of non-polar organic compounds that consist of two or more fused benzene rings in different chemical configurations including alkylated forms. These compounds are classified as organic pollutants because of their chemical stability and non-biodegradability. Additionally, PAHs are considered toxic, carcinogenic, mutagenic substances. For these reasons, there are numerous studies on PAHs in water, soil, and air [101]. According to the United States Environmental Protection Agency (US EPA), sixteen PAHs are priority pollutants (Table 1.6) based on their toxicity, human exposure and existence in waste sites. Seven of these PAHs, i.e., chrysene, benzo(a)anthracene, dibenzo(a,h)anthracene, benzo(a)pyrene, benzo(k)fluoranthene, benzo(b)fluoranthene, and indeno(1,2,3-cd) pyrene, are identified as probable human carcinogens. The carcinogenic PAHs typically have higher molecular weights, lower water solubility, and lower vapor pressure compared with non-carcinogenic PAHs [102]. PAHs with 2-4 benzene rings are considered light PAHs, and heavy PAHs contain 4 to 8 aromatic rings.

Table 1.5 US EPA 16 priority-pollutant PAHs

PAHs	Number of rings	Molecular weight (g/mole)	Solubility (mg/L)	Vapor pressure (mm Hg)
Naphthalene	2	128.17	31	8.89×10^{-2}
Acenaphthene	3	154.21	3.8	3.75×10^{-3}
Acenaphthylene	3	152.20	16.1	2.90×10^{-2}
Anthracene	3	178.23	0.045	2.55×10^{-5}
Phenanthrene	3	178.23	1.1	6.80×10^{-4}
Fluorene	3	166.22	1.9	3.24×10^{-3}
Fluoranthene	4	202.26	0.26	8.13×10^{-6}
Benzo(a)anthracene	4	228.29	0.011	1.54×10^{-7}
Chrysene	4	228.29	0.0015	7.80×10^{-9}
Pyrene	4	202.26	0.132	4.25×10^{-6}
Benzo(a)Pyrene	5	252.32	0.0038	4.89×10^{-9}
Benzo(b)fluoranthene	5	252.32	0.0015	8.06×10^{-8}
Benzo(k)fluoranthene	5	252.32	0.0008	9.59×10^{-11}
Dibenz(a,h)anthracene	6	278.35	0.0005	2.10×10^{-11}
Benzo(g,h,i)perylene	6	276.34	0.00026	1.00×10^{-10}
Indeno[1,2,3-cd]pyrene	6	276.34	0.062	1.40×10^{-10}

1.6.1 Sources, classification and distribution of PAHs

PAHs are widely distributed in the natural environment such as water, soil, sediments, air, plants, and animals. Their generation can be grouped as pyrogenic and petrogenic, which can be associated with natural processes or enter the environment through human

activities. Pyrogenic sources include forest fires, natural oil seeps and volcanic eruptions. Petrogenic are, by definition, compounds from fossil fuels, however other industrial processes, such as, waste incineration can be point sources for the discharge of petrogenic compounds as well. PAHs can reach the atmosphere mostly through gaseous emissions but also through evaporation or particulate inputs from soil and water. PAHs are mainly discharged into aquatic systems via natural oil seeps or from oil extraction activities [101, 103-105]. Due to their low solubility, heavy PAHs in water can bind to sediments and suspended particulate or accumulate in aquatic animals. Light PAHs, on the other hand, are more water soluble, making them detectable and extractable from aqueous system [61].

1.6.2 Analytical methods for detection of PAHs

Detection of PAHs in the environment has been an important topic for decades due to their high potential for adverse health effects. Monitoring PAHs in the marine environment was initiated in the 1960s, and today this continues on a range of regional and local scales [106]. The major long-term PAHs monitoring projects, which mainly focus on marine environments, include the Baltic Marine Environment Protection Commission (Helsinki Commission), the Arctic Monitoring and Assessment Program (AMAP), and the National Status and Trends Program (US) [107-109].

Detection and quantification of PAHs in environmental media tend to be difficult because of the complexity of environmental samples. These samples can be in different phases

such as gaseous, solid (biological samples), liquid (water, oil or organic liquids) samples [110]. Therefore, reliable analytical methods are essential for detection of PAHs in these samples. Chromatographic methods for detection of PAHs in environmental matrices have been widely used and improved tremendously over the past few decades [107, 111]. The US EPA predominantly applies liquid chromatography (LC) and gas chromatography (GC) techniques for monitoring PAHs in a range of samples such as municipal and industrial discharges, drinking water, solid waste, living tissue and ambient air [112-116].

At the National Institute of Standards and Technology (NIST), the 16 US EPA PAHs, plus other PAHs, are measured in environmental reference materials using LC and GC coupled to a range of acceptable detection techniques to improve selectivity and sensitivity as well as to provide detection of a wide range of analytes [117]. For example, anthracene and perylene can selectively and sensitively be detected by fluorescence spectroscopy [118]. Low concentrations of these PAHs are successfully measured by use of LC coupled with fluorescence detection (LC-FL) [111]. In contrast, benzo[g,h,i]perylene, which is very weakly fluorescent, can be more sensitively and accurately measured by GC coupled with mass spectrometry (GC-MS) [119]. A recent advancement in detecting complex samples utilized the strengths of both LC and GC. In this LC-GC method, the sample is separated by LC and the individual fractions analyzed by GC-MS to achieve high selectivity and low detection limits [120].

1.7 Research goals

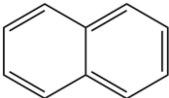
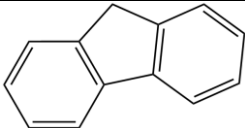
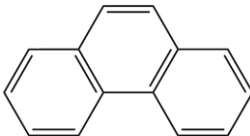
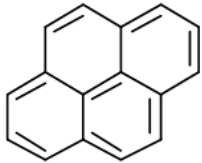
The first objective of this research was to develop a system to characterize the factors influencing the porosity in MIP synthesis using a parametric study of solubility and phase separation. MIPs used as sorbents or as sensing materials must have high porosity that is uniform with reproducible morphological features. The porogen plays a crucial role in the realization of MIP properties such as surface area, pore volume, and pore size. Therefore, a strategy used for traditional porous polymer synthesis was adopted to choose a suitable porogen to prepare a novel thin film MIP with desired properties. In this method, the Hansen solubility parameters of polymers were calculated using a numerical model in Matlab which is described in Chapter 2. The Hansen solubility parameters account for a range of interactions between a solvent and a solute and can be used practically to predict the thermodynamic compatibility of a porogen with a polymeric network so that conditions can be selected to produce a macroporous polymer without trial and error porogen optimization.

The second goal of this research was to test the MIP thin films developed in light of HSP-based optimization in a method for analysis of light PAHs (naphthalene, fluorene, phenanthrene, and pyrene, Figure 1.7) in water samples using GC-MS. These PAHs are most commonly found in the dissolved phase of produced water. Validation of the MIP analysis method for extraction of PAHs from aqueous PAHs solutions was obtained through evaluation of selectivity and sensitivity at low upload concentrations and in different upload times. In addition, kinetic studies of adsorption PAHs by MIPs were done through

various binding experiments, which are described in Chapter 3. In addition, the suitability of MIPs for environmental analysis and complex aqueous samples was tested in produced water with no sample preparation. The results revealed excellent sensitivity, selectivity and linearity, suggesting that MIPs can be successfully used for analysis of real aqueous samples in the environment.

Table 1.7 shows four target molecules were studied in this work.

Table 1.6 Target molecules focused on in this work

Compounds	Structure	Molecular weight	Solubility in water (mg/L) at 25 °C
Naphthalene		128	32
Fluorene		166	1.9
Phenanthrene		178	1-1.3
Pyrene		202	0.14

Chapter 2. Theoretical and Experimental Methods for Selection of Porogen for MIPs Fabrication

2.1 Introduction

MIPs are smart polymers for selective recognition of target solutes [121, 122]. As with most porous adsorbents, MIPs should exhibit high surface area and porosity, controlled pore size and mechanical stability [123]. It is recognized that the solvent plays a key role in a pore generation, influencing shape, size and volume of pores in MIPs [66, 124, 125]. Whether a solvent acts as a true porogen will depend on its thermodynamic compatibility with the functional monomer, cross-linker and template [73]. This is because the thermodynamic compatibility significantly affects the phase separation and polymer properties [126]. Hansen's three-dimensional solubility parameter is a practical criterion for predicting the thermodynamic compatibility of a porogen with the prepolymerization components, as well as the propensity to form a polymeric network with the required characteristics [36, 127, 128]. Rather than take a trial-and-error approach, we used Hansen solubility parameters to develop a numerical method to predict the suitability of a porogen for formation of an MIP film with specified porosity.

2.2 Determination of poly(methacrylic acid) HSP

2.2.1 Synthesis of cross-linked poly(methacrylic acid) (PMAA)

2.2.1.1 Materials

Methacrylic acid monomer, ethylene glycol dimethacrylate (EGDMA) cross-linker, potassium persulfate (KPS) thermal initiator were purchased from Sigma-Aldrich (Oakville, ON, Canada), compressed nitrogen gas and Whatman Quantitative filter papers (No. 89212.5 cm folded circles).

2.2.1.2 Method

The PMAA was synthesized by radical polymerization of a prepolymerization solution consisting of 170 μL of methacrylic acid (monomer), 0.03200 g of potassium persulfate ($\text{K}_2\text{S}_2\text{O}_8$), and 1510 μL of EGDMA in 10 mL of deionized water. Nitrogen gas was bubbled through the prepolymerization mixture for 10 min to remove any dissolved oxygen that would interfere with the polymerization reaction. Polymerization was carried out for 8 h at 60 °C. The resulting cross-linked PMAA material was immersed in water for 24 h to remove any unreacted materials. Polymer particles were collected on filter paper then dried in a vacuum oven at 35 °C until a constant weight was achieved.

2.2.2 Swelling test of Cross-linked PMMA

2.2.2.1 Materials

Several representative solvents, including protic, aprotic, polar and non-polar, were used in the swelling experiments. Nonpolar solvents types included aromatic (benzene and toluene), aliphatic (hexane), cycloalkane (cyclohexane) and halomethane (chloroform). Polar solvents were subdivided into four groups: ketone (acetone), ether (tetrahydrofuran (THF)), ester (ethyl acetate) and nitrile (acetonitrile). Protic solvents that are good at forming hydrogen bonds in the solvation process were represented by alcohols (methanol, ethanol, 1-octanol, cyclohexanol, benzyl alcohol). All solvents with purity greater than 95% were obtained from ACP Chemicals (Montreal, QC, Canada).

2.2.2.2 Method

The swelling test was carried out by immersing 5.00 mg of PMAA in a beaker containing 100 mL of solvent for up to 10 hours. At 1-h intervals, a portion of polymer was removed from the solvent, dried at room temperature and weighed to five decimal places.

2.2.2.3 Results and discussion

Hansen solubility parameters of highly cross-linked (insoluble) polymers are usually measured through swelling tests [129], where upon swelling the solvent diffuses into the polymer pore structure. The amount of solvent retained by the polymer is indicative of its interaction with the polymer and can be detected by a change in mass associated with the

retained solvent. The results of the swelling tests are used to determine the HSP values for a given polymer system. The swelling value can be estimated by using the following formula:

$$\text{Swelling (\%)} = (W_s - W_d) / W_d \times 100 \quad (2.1)$$

where W_d is the weight of the polymer and W_s is the weight of the swollen polymer.

Figure 2.1 illustrates the effect of contact time on the swelling of PMAA. Benzyl alcohol, THF, chloroform, cyclohexane, acetone, acetonitrile and ethyl acetate have high swelling percentages, indicating a strong interaction with the polymer.

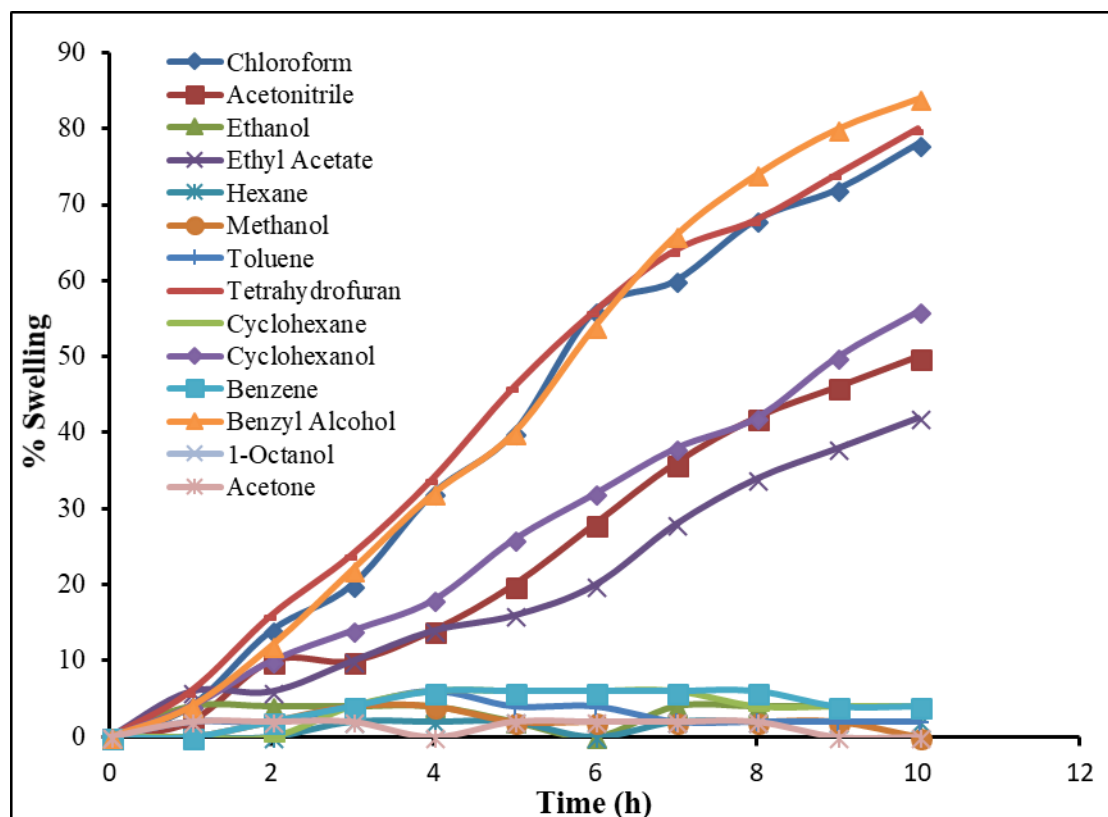


Figure 2.1 The effect of contact time on the percent swelling of PMAA

The strength of the interactions between PMMA and ethanol, methanol, hexane, toluene, cyclohexane is negligible, as shown in the very low percent swelling. Any solvent that can swell the PMAA is given a swelling factor equal to 1; the swelling factor is assigned as 0 for those solvents which could not swell the polymer. The HSP data for the solvents and the swelling factor assignments used in the calculations of HSP for the PMMA can be seen in Table 2.1.

Table 2.1 HSP values of solvents and swelling factor for PMMA

Solvents	$\delta_d(\text{MPa})^{1/2}$	$\delta_p(\text{MPa})^{1/2}$	$\delta_h(\text{MPa})^{1/2}$	Swelling Factor	%Swelling (10 h)
Chloroform	17.8	3.1	5.7	1	78
Acetonitrile	15.3	18.0	6.1	1	50
Ethanol	15.8	8.8	19.4	0	4
Ethyl Acetate	15.8	5.3	7.2	1	42
Hexane	14.9	0	0	0	2
Methanol	14.7	12.3	22.3	0	0
Toluene	17.6	1.4	2.0	0	2
Tetrahydrofuran (THF)	16.8	5.7	8.0	1	80
Cyclohexane	16.8	0	0.2	0	4
Cyclohexanol	17.4	4.1	13.5	1	56
Benzene	18.4	0	2.0	0	4
Benzyl Alcohol	18.4	6.3	13.7	1	84
1-Octanol	17.1	3.3	11.9	0	0

2.2.3 Computation of the HSP for PMAA and application for solvent suitability

2.2.3.1 Calculation of PMAA HSP using Hansen algorithm and MATLAB Program

The Hansen algorithm (Figure 1.4) was used in MATLAB (R2013b) to determine the HSPs (δ_d , δ_p , δ_h) and R_o of PMAA. The specifics of the MATLAB script used in this work were published by Gharaghazi (Appendix 1) [46]. The HSPs and R_o calculated for PMAA are $\delta_d = 15.22$, $\delta_p = 16.18$, $\delta_h = 1.97$, $R_o = 16.63$.

2.2.3.2 RED values for porogenic solvents: compatibility assessment

RED values were calculated using Equation 1.11. When the RED value is less than 1.0 the corresponding solvent has a higher affinity for the polymer. Therefore, it should be able to dissolve the polymeric network or swell highly cross-linked polymers. Such solvents are called *good* solvents and lie within the Hansen sphere. When the RED is larger than 1.0, the solvent has lower interaction with the polymeric network and it cannot dissolve or swell the polymer; thus it is considered a poor solvent [130, 131]. Table 2.2 shows the calculated R_a and RED values for solvents that were used in the swelling experiments. As can be seen, chloroform, acetone, acetonitrile, ethyl acetate, hexane, tetrahydrofuran, cyclohexane and benzyl alcohol have RED values below 1.0. These solvents are inside the Hansen sphere, which is depicted in Figure 2.2. Ethanol, methanol, toluene, cyclohexanol, benzene and 1-octanol have RED above 1.0, which excludes them from the Hansen sphere. Among all the solvents used in the swelling test, 1-octanol has RED = 1.014, which is very close to the boundary condition (RED = 1.0). At the boundary, the

growing polymer is moderately well solubilized and phase separation is neither late nor early. Therefore, we predicted that using 1-octanol as a porogen for fabrication of MIPs with methacrylic acid would result in polymers with favorable morphology and porosity.

Table 2.2 Calculated RED and R_a values for solvents used in the swelling tests.

Solvents	RED	R_a	$\delta_d(\text{MPa})^{1/2}$	$\delta_p(\text{MPa})^{1/2}$	$\delta_h(\text{MPa})^{1/2}$
Chloroform	0.875	14.551	17.8	3.1	5.7
Acetone	0.462	7.683	15.5	10.4	7.0
Acetonitrile	0.271	4.506	15.3	18.0	6.1
Ethanol	1.1403	18.963	15.8	8.8	19.4
Ethyl Acetate	0.729	12.123	15.8	5.3	7.2
Hexane	0.981	16.314	14.9	0	0
Methanol	1.246	20.720	14.7	12.3	22.3
Toluene	1.394	23.182	17.6	1.4	2.0
Tetrahydrofuran (THF)	0.751	12.489	16.8	5.7	8.0
Cyclohexane	0.897	14.917	16.8	0	0.2
Cyclohexanol	1.098	18.259	17.4	4.1	13.5
Benzene	1.445	24.030	18.4	0	2.0
Benzyl Alcohol	0.989	16.447	18.4	6.3	13.7
1-octanol	1.014	16.862	17.1	3.3	11.9

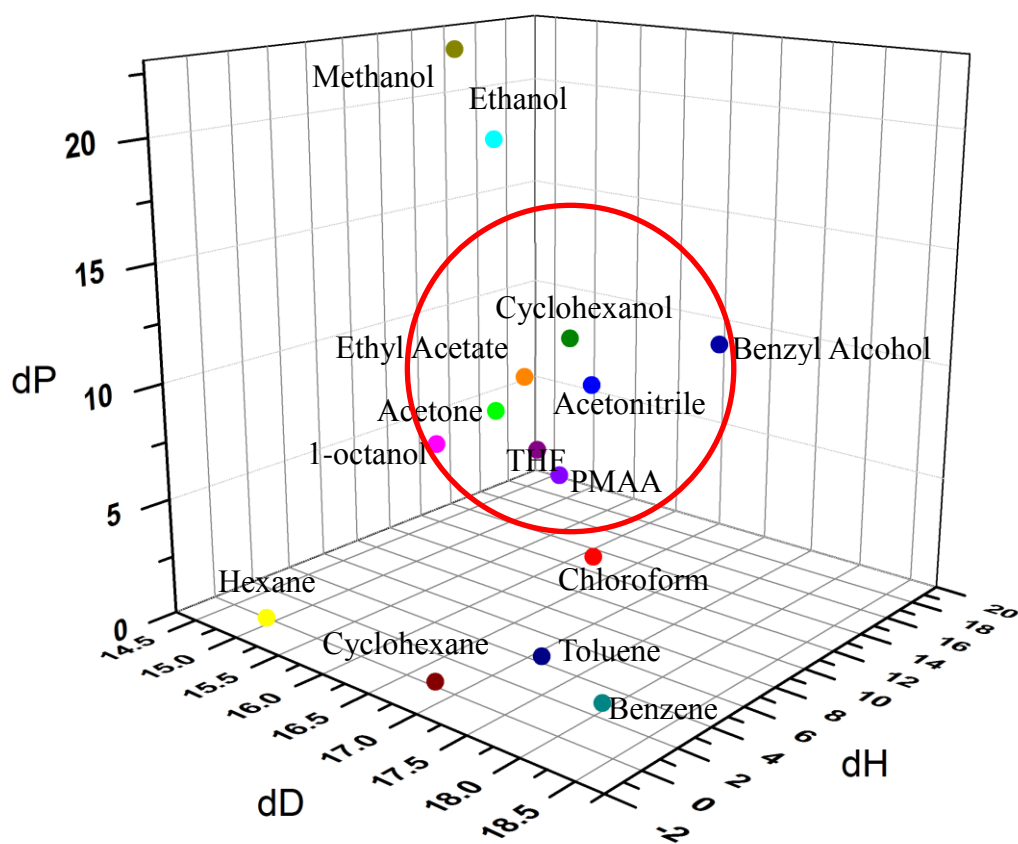


Figure 2.2 Hansen Space of PMAA. The red circle denotes the Hansen sphere for PMAA.

2.3. Effect of porogen type on thin-film MIPs

2.3.1 Materials

Compounds used in the preparation of the thin-film MIPs: MAA (monomer); EGDMA, (cross-linker); phenol (pseudo-template); 3-(trimethoxysilyl)propyl methacrylate (derivatizing agent for the glass substrate); and the 2,2-dimethoxy-2-phenylacetophenone (DMPA), initiator (Figure 2.3 and Table 2.3), were purchased from Sigma-Aldrich (Oakville, ON, Canada) and were used without further purification.

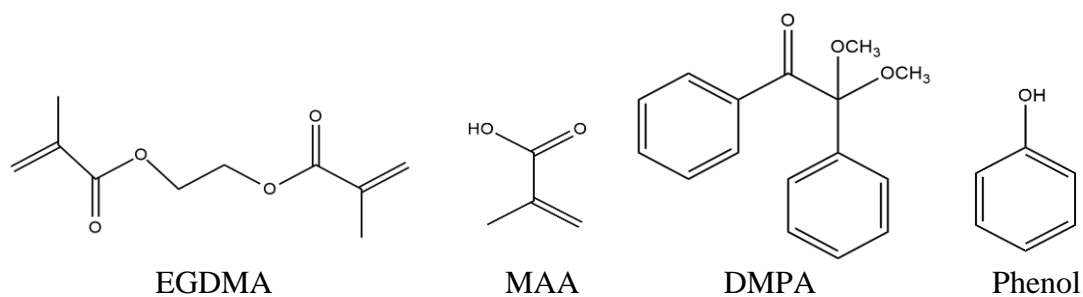


Figure 2.3 MIP components structures

Table 2.3 MIP and NIP composition

Pre-polymer component	MIP	NIP
1-octanol:methanol (80: 20 v/v) (porogen)	1-octanol 160 μ L methanol 40 μ L	1-octanol 160 μ L methanol 40 μ L
Phenol (pseudo-template)	0.0038 g	-
Methacrylic acid (MAA) (monomer)	13.33 μ L	13.33 μ L
Ethylene glycol dimethacrylate, 1,4 divi- nylbenzene (EGDMA) (cross-linker)	151 μ L	151 μ L
2,2-Dimethoxy-2-phenylacetophenone (DMPA) (photo-initiator)	0.0032 g	0.0032 g

2.3.2 Methods

2.3.2.1 Derivatization of glass slide

Before derivatization, glass microscopic slides (purchased from Bio Nuclear Diagnostics Inc) were washed with a mixed solution of HCl and methanol then rinsed with methanol

and water. For derivatization, cleaned glass slides were kept overnight in the solution of 2.0% of 3-(trimethoxysilyl)propyl methacrylate in toluene, rinsed with ethanol, dried under N₂ gas and covered in aluminum foil to avoid light.

2.3.2.2 Fabrication of thin-film MIP and NIP

The pre-polymerization components were transferred into a 2-mL vial and vortexed until dissolved, which yields the pre-polymerization complex. The solution was degassed for 5 min to remove oxygen that may react as a radical inhibitor during polymerization. Then 8.0 μ L of solution was dispensed onto a derivatized glass slide and quickly covered with a glass microscope slide cover. The solution was sandwiched between the microscope slide and the cover slide and was exposed to UV light (6 W, 254 nm) for 30 min to initiate polymerization. The cover slide was removed after polymerization to leave a solid polymer on the microscope slide substrate. The pseudo-template and unreacted species were extracted by stirring in methanol/acetic acid (9:1, v/v) for 2 h.

2.3.2.3 Characterization of MIPs

The porosity and surface morphology MIPs were assessed using scanning electron microscopy (SEM). SEM images were recorded using a FEI MLA 650F SEM, operating at an accelerating voltage of 10 kV and a magnification of 50,000 times. All samples were coated with gold before analysis.

2.3.3. Results and discussions

MIP thin films were prepared using porogenic solvents with different RED values. Acetonitrile, chloroform, benzyl alcohol with RED values 0.271, 0.875 and 0.989, respectively, were used as solvents located within the sphere and considered as *good* thermodynamic solvents. These thermodynamically porogens should solvate the copolymeric network well. The lowest RED values mean that the solvent will solvate the polymer system most effectively, hence; phase separation should be late, leading to microporous morphologies, which are typically glassy or gel-like polymers [3] .

Pictures of the MIPs fabricated on the glass slides using different porogenic solvents by various RED values are presented in Figure 2.4. As Figure 2.4 a illustrates, a transparent polymer is formed with acetonitrile as the porogen. Acetonitrile has RED=0.271 which is considered as a *good* thermodynamic solvent for the PMAA network hence; a transparent glassy polymer is formed. It should also be noted that the film formed is more membrane-like and detaches from the glass surface easily, making an unstable coating. Chloroform with RED = 0.875 (Figure 2.4 b) also is a “good” solvent for PMAA and this should also produce a microporous system, though with earlier phase separation than the acetonitrile. Macroporous structures typically manifest as more opaque coatings, and this phenomenon is visible, but the film is quite inhomogeneous. Benzyl alcohol with RED=0.989, is included among solvents with good thermodynamic compatibility. Compared to acetonitrile and chloroform, its RED value is closer to the boundary condition (RED=1) which causes formation of MIPs with more homogeneous

structures, however; the appearance of the films (variable transparency) show that the thickness of polymer is not uniform (Figure 2.4 c) [30].

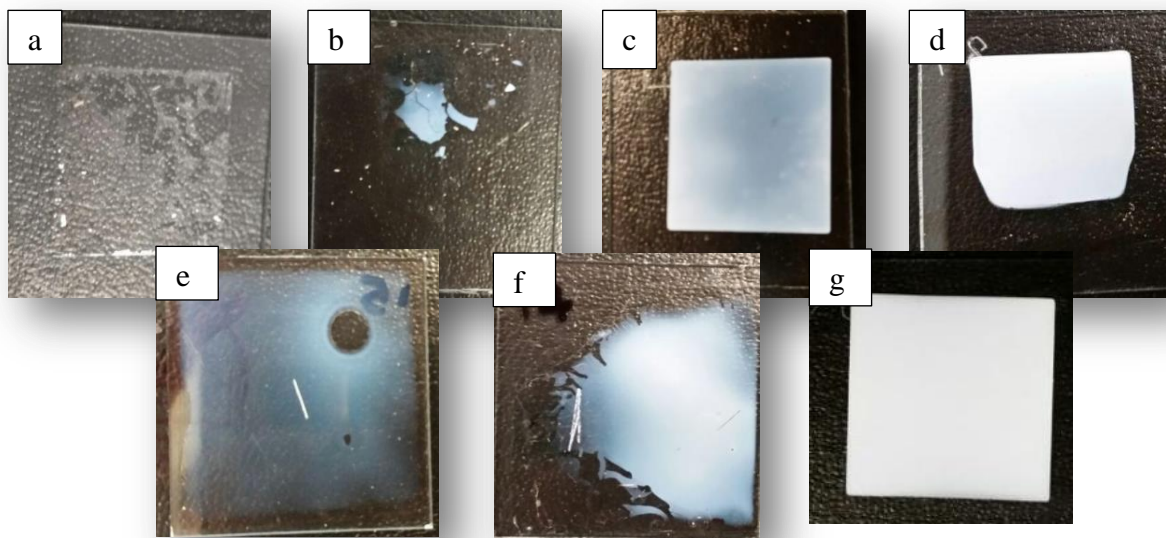


Figure 2.4 MIP slides prepared using different porogenic solvents: a) acetonitrile (RED = 0.271), b) chloroform (RED = 0.875), c) benzyl alcohol (RED = 0.989), d) 1-octanol (RED = 1.014), e) methanol (RED = 1.246), f) toluene (RED = 1.394), g) 1-octanol and methanol (v/v 80/20) (RED = 0.998).

Methanol and toluene have RED values 1.246 and 1.394 respectively, which are located outside the Hansen's sphere and are considered thermodynamically poor solvents [34]. In contrast with good solvents, these solvents do not solubilize the polymeric network well and they lead to very early phase separation, which can result in non-uniform

polymer films with irregular morphologies (Figure 2.4 d and e) [30]. On the other hand, 1-octanol ($RED = 1.014$) is close to the boundary condition and in this work produces opaque MIP thin films with a relatively uniform shape and good morphology (Figure 2.4 f). According to Figure 2.4, polymers formed on the glass slide using benzyl alcohol and 1-octanol have better shape and homogeneity in comparison with other solvents. The polymer fabricated with benzyl alcohol is not of good quality, though it has uniform edges. On the other hand, the polymer form with 1-octanol is quite homogeneous and opaque, but does not have uniform edges. These solvents have RED values close to the boundary condition. As reported in the data in Table 2.2, these two solvents have dispersion forces in the same range ($18.4 \text{ MPa}^{1/2}$ for benzyl alcohol and $17.1 \text{ MPa}^{1/2}$ for 1-octanol), their polarity is low ($6.3 \text{ MPa}^{1/2}$ for benzyl alcohol and $3.3 \text{ MPa}^{1/2}$ for 1-octanol) and they have moderate hydrogen bonding forces ($13.7 \text{ MPa}^{1/2}$ for benzyl alcohol and $11.9 \text{ MPa}^{1/2}$ for 1-octanol). Nevertheless, although much better than the other solvents tested, the films produced using 1-octanol still lack uniformity at the edges; it should be possible to improve this through application of HSPs in modification of the solvent system.

The HSPs and the resulting RED values should be suitable for the determination of the compatibility or incompatibility of the copolymeric network and a given porogen. Using this understanding as a guide along with the observations that HSPs and RED values can be fine-tuned using mixed solvent systems, experiments were carried out to develop a solvent system that is closer to the boundary condition ($RED = 1$). Starting with 1-octanol, as it gave the best results of those tested, HSPs and RED values for binary solvent systems were calculated in MATLAB (Appendix B). A selection of values is shown

in Table 2.4. It was observed that mixed solutions of 1-octanol and methanol (v/v 80/20) gives an RED value 0.998, which is very close to the boundary condition. To test the theory that this should improve the film characteristics, a MIP film was fabricated with excellent results; see Figure 2.4 g which depicts the film with a good uniformity along the edge.

The morphology and porosity of these MIP thin-films were further characterized by SEM, with the results produced in Figure 2.5. The film formed using toluene (RED=1.394, poor thermodynamic porogenic solvent) had an irregular surface with very low porosity. The porosity of MIPs improved in the presence of benzyl alcohol (RED=0.989, good thermodynamic porogenic solvent) however the particles show higher aggregation than desired (Figure 2.5 b). The surface of 1-octanol MIP showed high porosity and homogeneity (Figure 2.5 c). The SEM image in Figure 2.5 d show that the mixed 1-octanol and methanol (%v/v 80/20) solvent system yields MIPs with improved morphology consisting of macroporous and microporous features (Figure 2.5).

Table 2.4 RED value and HSPs of mixed solvents

	RED	$\delta_d(\text{MPa})^{1/2}$	$\delta_p(\text{MPa})^{1/2}$	$\delta_h(\text{MPa})^{1/2}$
PMAA	-	15.22	16.18	1.97
Mixed solvent system 80/20 (v/v)				
1-octanol/chloroform	0.907	17.2	3.3	10.7
1-octanol/acetone	0.894	16.8	4.7	10.9
1-octanol/acetonitrile	0.818	16.7	6.	10.74
1-octanol/ethanol	1.1	16.84	4.40	13.40
1-octanol/ethyl acetate	0.944	16.84	3.7	10.96
1-octanol/hexane	0.948	16.66	2.64	9.52
1-octanol/methanol	0.998	16.6	5.1	13.9
1-octanol/toluene	0.960	17.2	2.64	9.52
1-octanol/tetrahydrofuran	0.953	17.04	3.78	11.12
1-octanol/cyclohexane	0.959	7.04	2.6	2.6
1-octanol/cyclohexanol	1.02	17.16	3.46	12.22
1-octanol/benzene	0.978	17.36	2.64	9.92
1-octanol/benzyl alcohol	0.906	17.36	3.96	12.26

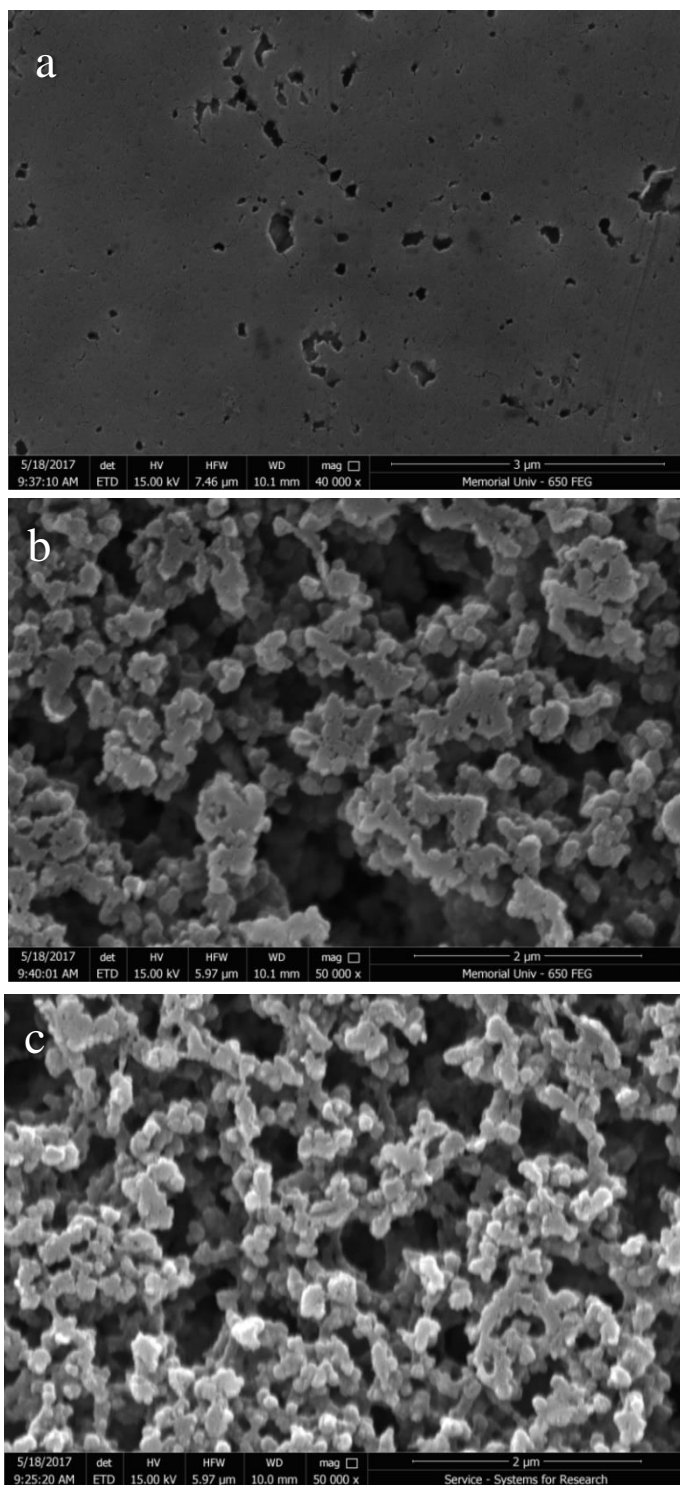


Figure 2.5(a-c). SEM image of MIP fabricated using a) toluene, b) benzyl alcohol and c) 1-octanol.

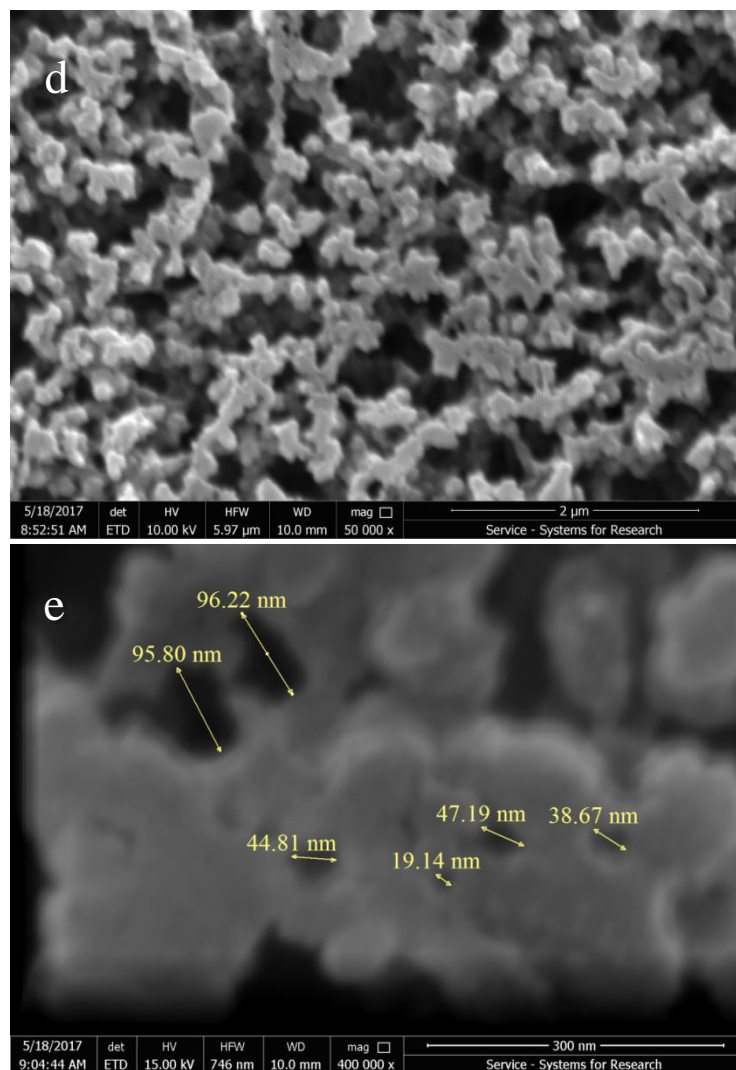


Figure 2.5(d,f). SEM image of MIP fabricated using d) 1-octanol/methanol (80/20 v/v)
e) pore details and sizes of d.

2.4 Conclusions

MIPs fabricated using a porogenic solvent with properties that place it at the boundary between good and poor porogens are stable, uniform, porous polymer films with uniform morphology. A porogenic solvent has properties that may help to control the phase separation of the polymer and chain growth. Poor solvents cause early phase separation of the polymer, which results in short chain polymers and unstable films with lack of porosity. In contrast, good solvents solvate the polymer system most effectively, hence; phase separation may be late, resulting in formation of microporous morphologies of glassy or gel-like polymers. Therefore, the optimum porogenic solvents for fabrication MIPs should be located at the boundary condition which is determined by calculating RED values.

Chapter 3. Using MIPs for Extraction of PAHs from Water Samples

3.1 Introduction

PAHs, a large class of non-polar organic compounds, consist of two or more fused benzene rings that are organized in different configurations. Chemically stable and slow to photo- or biodegrade, these compounds are classified as organic pollutants because of their toxicity, carcinogenicity and mutagenicity [132]. PAHs with 2-4 benzene rings, frequently alkylated, are mostly released into the environment from petrogenic sources (*e.g.* fossil fuels, industrial waste incineration), discharge of produced water and spills of petroleum products [133-136]. Depending on physical and chemical properties (the molecular weight, solubility and hydrophobicity), PAHs are ultimately found in soil, air, ground water, vegetation and oceans [137-140]. Light PAHs in seawater are an indicator of petroleum contamination in water, which is related to the oil extraction and consequently the discharge of produced water. For these reasons, there are an abundance of studies to develop methods for detection of PAHs in water, soil and air [141-143].

MIPs are a good choice for these methods because of their inherent selectivity. As with most porous adsorbents, MIPs should exhibit high surface area and porosity, controlled pore size and mechanical stability [30, 143]. In this work, we focused on developing MIPs for detection PAHs such as naphthalene, fluorene, phenanthrene and pyrene in seawater. In comparison to biologically-derived selective sorbents (*i.e.*, immunosorbents),

MIPs have advantages, such as chemical and physical stability, straight forward and low cost of preparation, and the ability to be designed to recognize a range of small molecules. In this work, a highly porous MIPs were prepared with MAA, EGDMA, phenol (pseudo-template), and 80:20 v/v 1-octanol/methanol as the porogen. In this case, pseudo-template imprinting based on phenol was used to avoid any issues associated with residual template left after template removal; it is difficult to remove all traces of the template, therefore false positives associated with template bleeding is possible. [61]. Phenol was used as pseudo-template because of its aromatic character, which is similar to the target molecules, and according to Dickert et al., using pseudo-template smaller than the target molecule can enhance the adsorption of target analytes [144].

To evaluate the selectivity of the MIPs, non-imprinted polymer films (NIPs) were also prepared with the same composition as the MIPs but in the absence of a template. NIPs were studied under the same experimental conditions as the MIPs. When MIPs and NIPs are exposed to a sample, the targeted analytes bind to MIPs and NIPs. Since MIPs have structures complementary with the target molecules in terms of shape and size, it should absorb the targets better than NIPs [145]. Uptake by NIPs can be used to approximate the non-selective interactions inherent in the material. The relationship between the MIPs and NIPs is expressed as the imprinting factor (IF) and is calculated in the following way:

$$IF = \frac{C_{MIP}}{C_{NIP}} \quad (3.1)$$

Where C_{MIP} is the concentration of an MIP bound analyte (usually expressed as mg/g polymer) and C_{NIP} is the concentration of an NIP bound analyte [104]. High IFs show the high selectivity of an MIP, which indicates a low level of nonspecific binding. The MIP would also show higher adsorption uptake or binding capacity (Q) because of the imprinting effect. Binding capacity is described as the amount of analyte bound per mass of adsorbent material. For instance, for an MIP it can be calculated as [86, 146]:

$$Q = \frac{mass(adsorbate)}{mass(MIP)} \quad (3.2)$$

Imprinting can be effectively studied using binding isotherms. A binding isotherm is a plot of binding capacities with respect to the adsorbate concentrations at constant temperature. Experimental binding isotherms can be modeled to better understand the binding regime and to determine which binding models apply to the system under study. The Freundlich isotherm is one of the most common binding models [147]. This isotherm describes the heterogeneity of binding sites and assumes that different sites have different adsorption energies. This binding model is presented as:

$$Q = K_f C^{1/n_f} \quad (3.3)$$

Where Q is the amount of analyte adsorbed per mass of the MIP, C is the concentration of free or unbound analyte, K_f shows the Freundlich constant that relates to the adsorption capacity, $1/n_f$, is the isotherm constant which describes strength of adsorption. Larger K_f and larger $1/n_f$ values show favorable interactions and higher adsorption.

It is recognized that the solvent system plays a key role in a pore generation, influencing shape, size and volume of pores in MIPs. As shown in Chapter 2, rather than taking a trial-and-error approach, we used Hansen solubility parameters to develop a method to predict the suitability of porogen for formation of a MIP film with specified porosity. The fabricated MIPs were used for detection of PAHs in water with quantitation of bound analytes measured with GC-MS in SIM mode. Binding studies carried out in both aqueous standard solutions and produced water samples show a linear response for MIPs and their corresponding non-imprinted polymers, NIPs. However, MIPs displayed superior selectivity and binding capacities for PAHs in water compared to NIPs. Binding isotherm studies support these conclusions.

3.2 Materials

Naphthalene (99%), fluorene (99%), phenanthrene (99.5%) and pyrene (99%) were used without any purification and were purchased from Sigma-Aldrich (Oakville, ON). Acenaphthene-d₁₀ (99 atom % D) was purchased from Isotec (Canton, GA). All organic solvents (toluene, methanol, dichloromethane, acetonitrile, 1-octanol and acetic acid) were purchased with minimum 99.5% purity from ACP Chemicals.

3.3 Methods

3.3.1 Adsorption experiments

A multi-standard stock solution of PAHs was made at a concentration of 100 mg/L by dissolving approximately 10 mg each of naphthalene, fluorene, phenanthrene, and pyrene in 100 mL acetonitrile. All solutions used to build calibration curves and for sorption experiments (uploading) were prepared from the stock solution by dilution in deionized water. Acenaphthene- d_{10} was selected as the internal standards due to its similarity to the target PAHs. The internal standard was prepared using approximately 10 mg of acenaphthene- d_{10} in 100 mL acetonitrile, followed by dilutions in dichloromethane to gain the desired concentration. Note that acetonitrile is more environmentally-friendly, thus was used in the generation of the stock solutions and serial dilution, but DCM is more compatible with GC-MS.

For uploading experiments, thin-film MIPs and NIPs were separately immersed in 100.0 mL of aqueous PAH multi-standard solutions (various concentrations) at room temperature for specific time intervals with continuous stirring. The MIPs and NIPs were removed from the solution, rinsed with a small volume of distilled water and dried with nitrogen gas to remove visible water droplets. The target analytes were desorbed from the films in 10.0 mL of methanol under continuous stirring for two hours. The solvent was evaporated from the extracts with a stream of nitrogen; the residues were spiked with acenaphthene- d_{10} to give a concentration of 50 mg/L once the solution was made to volume with DCM in a 1-mL volumetric flask. The concentrations of PAHs in these solu-

tions were measured by GC-MS. These results were used to determine IF and binding isotherms. The effect of time also was considered by changing the uploading time. All calibration standards and extracts were prepared in replicates of three. The PAHs calibration curves were plotted using linear regression of data from analysis of multi-component solutions made in 6 concentrations from 10 to 100 mg/L for each PAH.

3.3.2 GC-MS Method

Analytes were analyzed with GC-MS with an Agilent 6890-5973 GC-mass selective detector MSD. The GC was fitted with a DB-5ms fused silica capillary column (30 m x 0.250 mm, 0.25 μ m stationary phase film thickness). Samples were deposited into the injection port at 290 °C, and transferred to the column in splitless mode with a He carrier gas at 1.3 mL/min. The oven temperature was first maintained at 45 °C held for 0.8 min, raised to 200 °C at 3 °C/min, raised to 216 °C at 5 °C/min and finally raised to 260 °C at 10 °C/min. The total time of analysis was 13.57 min. The separated bands were detected by MS in selective ion monitoring (SIM) mode, with an electron ionization (EI) ion source operated at 70 eV. The selected ions for the four PAHs and internal standard are listed in Table 3.1.

Table 3.1 GC-MS mode parameters used to identify the PAHs

Analyte	Primary ion (m/z)	Secondary ions (m/z)	SIM start time (min)
Naphthalene	128	127, 129	3.00
Acenaphthene-d ₁₀	164	158, 160, 162	6.00
Fluorene	166	139, 165, 167	6.50
Phenanthrene	178	152, 176, 179	7.50
Pyrene	202	101, 200, 203	10.50

3.4 Results and discussion

3.4.1 MIP fabrication

Based on a novel systematic method using Hansen solubility parameters, a suitable mixture of 1-octanol and methanol was selected as the porogen for fabrication of porous and opaque white thin-film MIPs. The procedure (Section 2.3.2.2) used for fabrication of thin-films MIPs is very simple, fast and uses low-tech equipment such as a vortex mixer, an ultrasonic bath and a UV-lamp. Morphology and porosity of imprinted polymers were characterized by SEM. Performance was evaluated using a range of binding studies to characterize uptake behavior and to assess analytical performance.

3.4.2. Binding studies of MIP for PAHs

A preliminary test of the selectivity and sensitivity of the PAH-MIPs and NIPs with the GC-MS instrumental method was carried out using a series of upload and extraction experiments of aqueous multi-PAHs solutions with concentrations ranging from 10.0-100 µg/L. Figures 3.1 (a-d) show the results of uploading to the MIPs and NIPs thin films expressed in terms of the peak area of analyte normalized to the peak area of internal standard (acenaphthene-d₁₀). The results are the mean value of three measurements. Both NIP and MIP should share some non-selective binding between the target molecules and the functionalized polymer. The slopes of the calibration curves show the sensitivity and affinity of MIPs is higher than that of the NIPs, which can be attributed to the presence of higher affinity imprinted sites. [133].

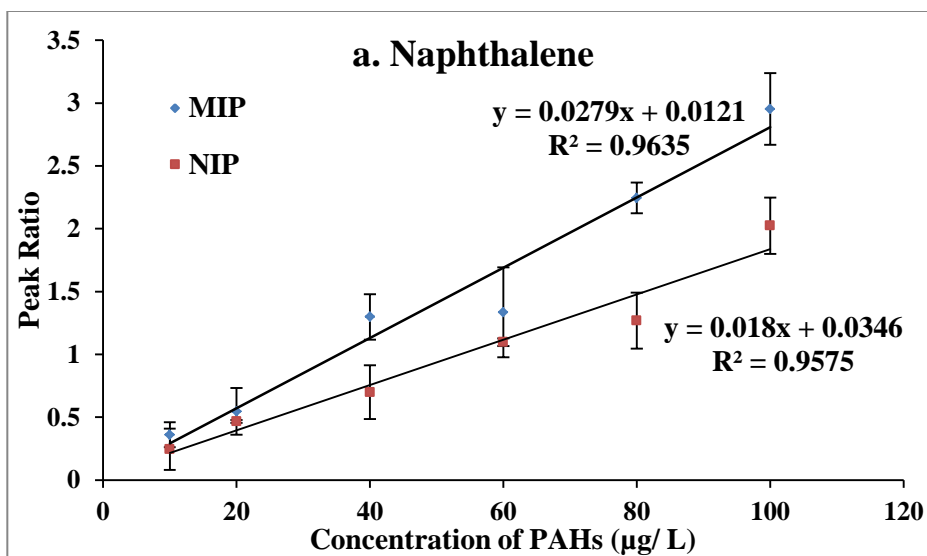


Figure 3.1a Calibration curve for extraction of a) naphthalene in aqueous multi-PAHs solutions using MIPs and NIPs with analysis by GC-MS in SIM mode.

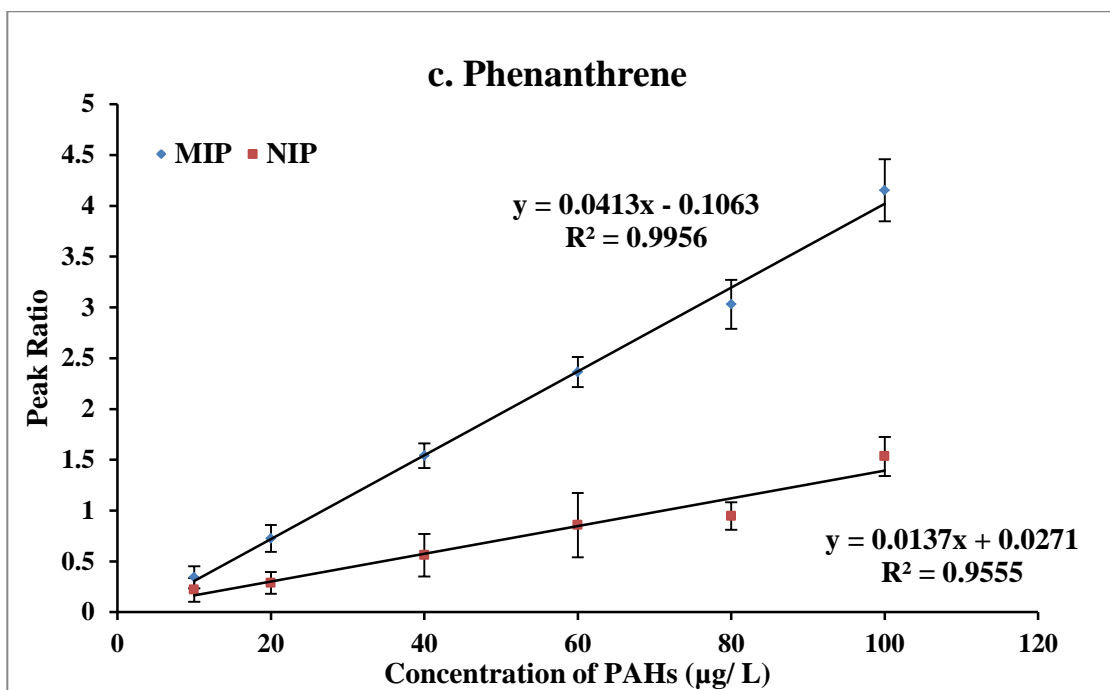
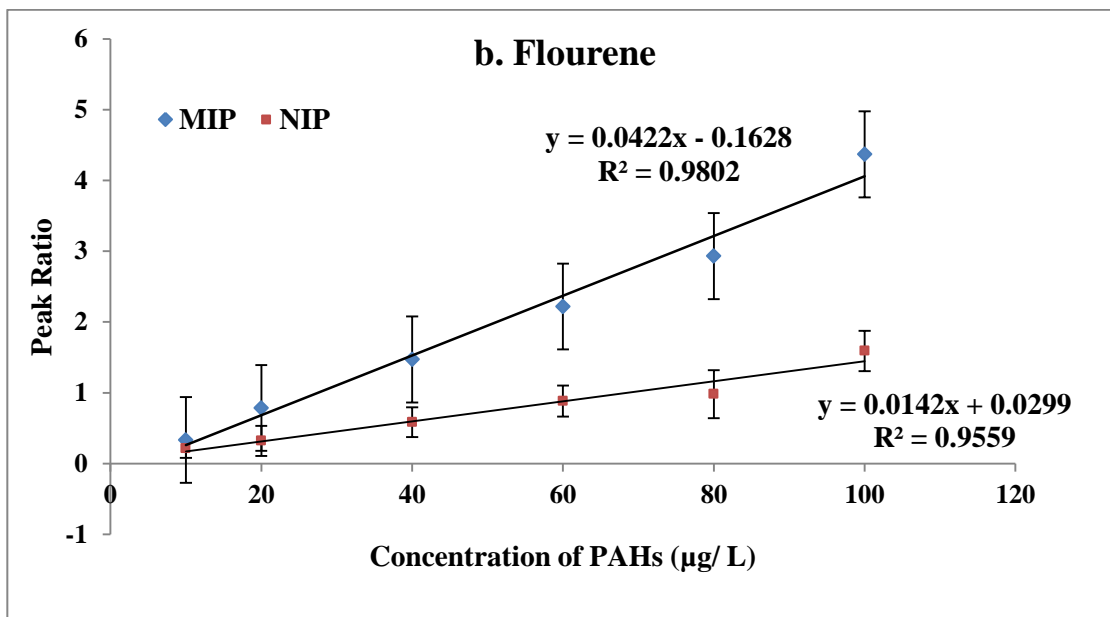


Figure 3.1(b,c) Calibration curve for extraction b) fluorene and c) phenanthrene in aqueous multi-PAHs solutions using MIPs and NIPs with analysis by GC-MS in SIM mode.

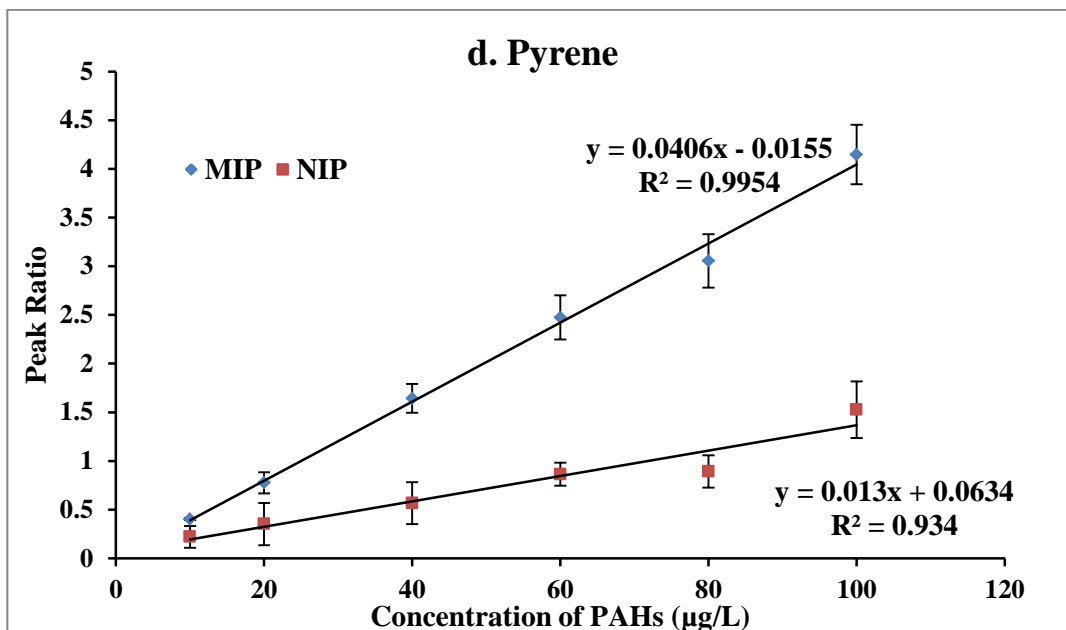


Figure 3.1d Calibration curve for extraction d) pyrene in aqueous multi-PAHs solutions using MIPs and NIPs with analysis by GC-MS in SIM mode.

All the curves show a strong linear relationship between the amount of analyte extracted and the initial concentration of PAHs in the standard solutions. The MIPs showed the highest sensitivity for pyrene and phenanthrene, followed by fluorene and naphthalene. This can be attributed, in part, to the hydrophobicity of the larger PAHs, but also includes binding to imprinted sites in the polymer network. The NIPs showed uptake even in the absence of the selective recognition sites, but uptake by the NIPs is lower than the MIPs, which confirms that the templating process imparts greater selectivity to the material.

At each concentration, the mean value of the imprinting factor (IF) was calculated and the results are presented in Table 3.2 along with the octanol-water partition coefficient.

cient (expressed as $\log K_{ow}$) as an indicator of hydrophobicity. The IF values for MIPs and NIPs were calculated using Equation 3.1. Table 3 shows that at all PAH concentrations the MIPs showed higher uptake than NIPs. The surface chemistry of the MIPs and NIPs make them suitable for adsorbed aromatic hydrocarbons through hydrophobic interactions [148]. Larger PAHs are more hydrophobic and there is a greater driving force for hydrophobic interactions and sorption with the polymer. It is expected that the high affinity sites are occupied first and might be saturated at high concentrations, which could result in higher IF values at low concentrations. This is consistent with performance others have reported for MIPs[149]. The increased uptake of the MIP compared to the NIP also demonstrates that the MIP will give more sensitive analytical results.

Table 3.2 Mean IF values obtained for PAHs adsorbed by MIPs in 10-100 ($\mu\text{g/L}$) concentration range with analysis by GC-MS in SIM mode.

Concentration ($\mu\text{g/L}$)	Naphthalene ($\log K_{ow}=3.37$)	Fluorene ($\log K_{ow}=4.18$)	Phenanthrene ($\log K_{ow}=4.5$)	Pyrene ($\log K_{ow}=5.18$)
10	1.47 \pm 0.05	1.56 \pm 0.04	1.57 \pm 0.10	1.83 \pm 0.04
20	1.16 \pm 0.05	2.45 \pm 0.08	2.52 \pm 0.13	2.21 \pm 0.08
40	1.85 \pm 0.20	2.52 \pm 0.18	2.75 \pm 0.23	2.90 \pm 0.33
60	1.22 \pm 0.32	2.51 \pm 0.08	2.77 \pm 0.11	2.87 \pm 0.07
80	1.77 \pm 0.09	2.99 \pm 0.15	3.21 \pm 0.36	3.45 \pm 0.51
100	1.45 \pm 0.26	2.75 \pm 0.10	2.71 \pm 0.26	2.72 \pm 0.27

3.4.3. Evaluation of adsorption properties of PAHs onto MIPs

3.4.3.1 Effect of time on the PAHs adsorption

Binding behavior, specifically equilibration time, of PAHs with MIPs was studied using 10.0 µg/L aqueous PAH multi-standard over a ~16-h interval. The amount of analyte extracted was determined by GC-MS analysis of analyte desorbed quantitatively from MIP films. From the data presented in Figure 3.2, it can be concluded that adsorption increases rapidly in the first 3 h, and that the system has neared equilibrium by 6 hours. Although, small increases in adsorption are seen over 16 h, the increase is not significant and would not improve detection limits substantially if used. Compared to other MIP systems studied in our group and by others (Figure 3.3 Song *et al.* [150]), equilibration appears to occur more rapidly for this system. The high adsorption rate can be due to the rapid and preferential adsorption of PAHs onto the specific binding sites in mesoporous MIPs; the slower phase of adsorption is related to a depletion of stronger binding sites and the time required for analyte to diffuse to active sites found within the nano-porous structure [151].

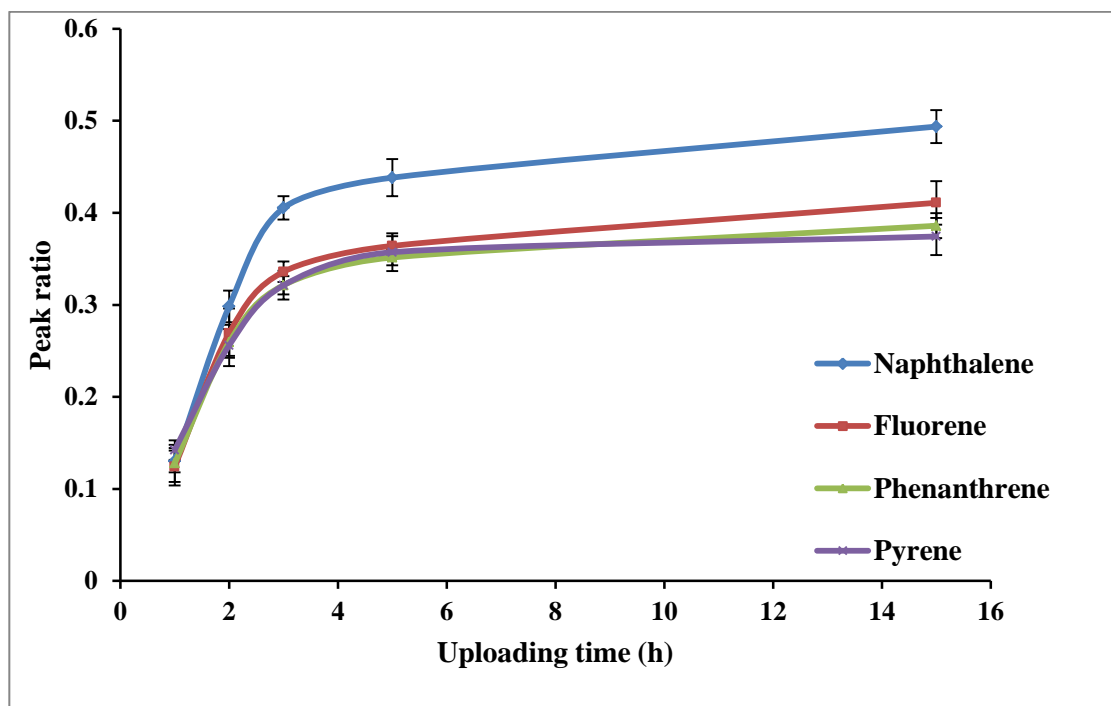


Figure 3.2 Time-dependent adsorption of naphthalene, fluorene, phenanthrene and pyrene onto the MIPs in 100 mL of 10 $\mu\text{g/L}$ each. Measured by GC-MS in SIM mode. Two replicates. Peak ratio: peak area of analytes/peak area of internal standard.

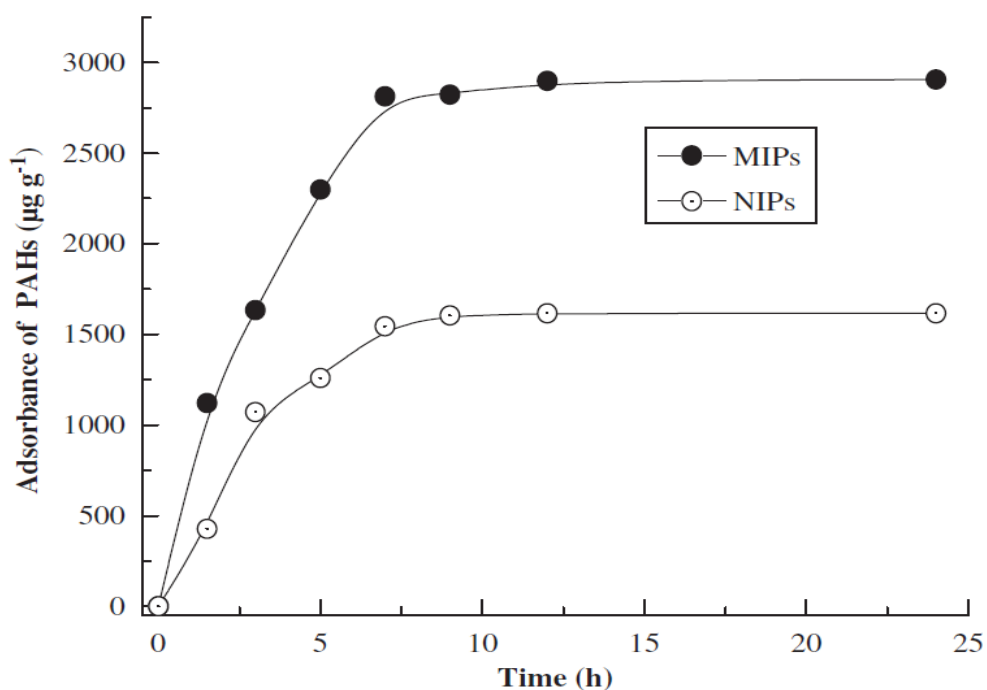


Figure 3.3 Binding of PAHs for MIPs and NIPs. Experimental conditions: $V=100.0$ mL; $C_0=1$ mg/L; mass of polymer=50 mg (used with permission from reference [150]).

3.4.3.2 Binding isotherm for MIPs/NIPs uploaded in PAHs solutions

Adsorption isotherm models are used to understand the fundamental characteristics of MIP binding properties [152]. These isotherms graph the adsorption behavior of the analyte toward the MIP relative to solution concentration; the shape of the graphs can give an indication of the homogeneity or heterogeneity of sorbent material. In this study, MIP binding behaviors were characterized through Freundlich adsorption isotherm of PAHs rebinding from aqueous solutions [147]. The imprinting effects of MIPs were evaluated

using Freundlich fitting parameters based on analysis of the PAHs binding isotherms. Figure 3.4 illustrates the results of fitting the data to the Freundlich isotherm for the four PAHs for MIPs and NIPs. Since there are various binding site distributions (specific and nonspecific) on the MIP, we applied the Freundlich isotherm model which describes heterogeneous adsorption processes. The Freundlich isotherm is defined by Eq. 3.4 [153].

$$Q = K_F C^{1/n_f} \quad (3.4)$$

The K_F and n_f are Freundlich fitting parameters, which are calculated using a MATLAB curve fitting algorithm, and are listed in Table 3.3. K_F is the Freundlich adsorption capacity constant, which shows the adsorption capacities of the MIPs and NIPs. The $1/n_f$ values describe the adsorption intensity of MIPs and NIPs. Where $0.1 < 1/n_f < 1.0$ indicates highly favorable adsorption, whereas; $1/n_f > 2$ denotes unfavorable adsorption. As the data shows, adsorption of PAHs by MIPs is more favorable than for NIPs due to the larger K_F and smaller $1/n_f$ value of MIPs than NIPs [153].

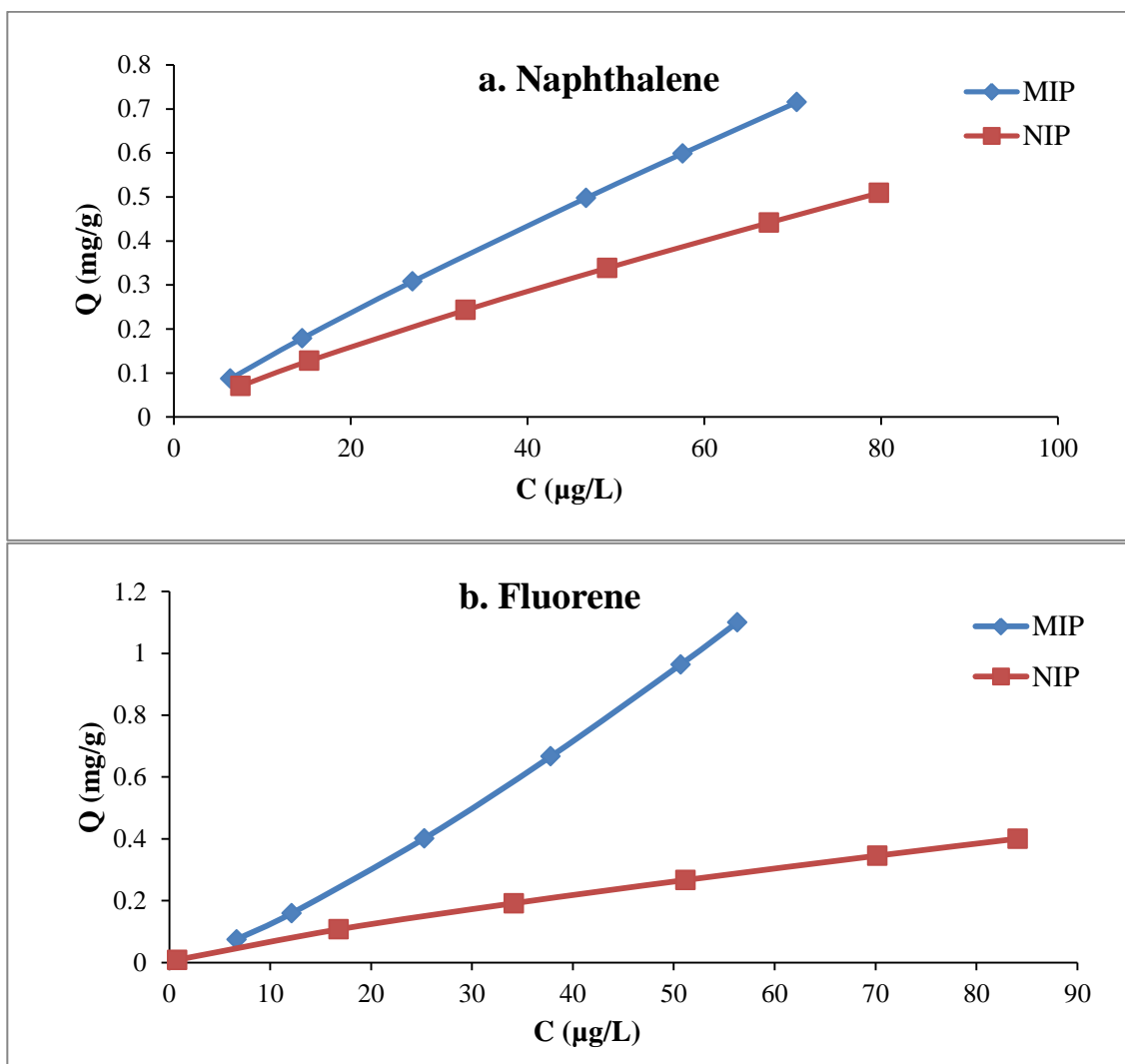


Figure 3.4(a,b) Freundlich binding isotherms graph for a) naphthalene and b) fluorene, adsorbed by for MIP/NIP uploaded in 100 mL of aqueous PAHs solution in 10-100 $\mu\text{g/L}$ concentration range.

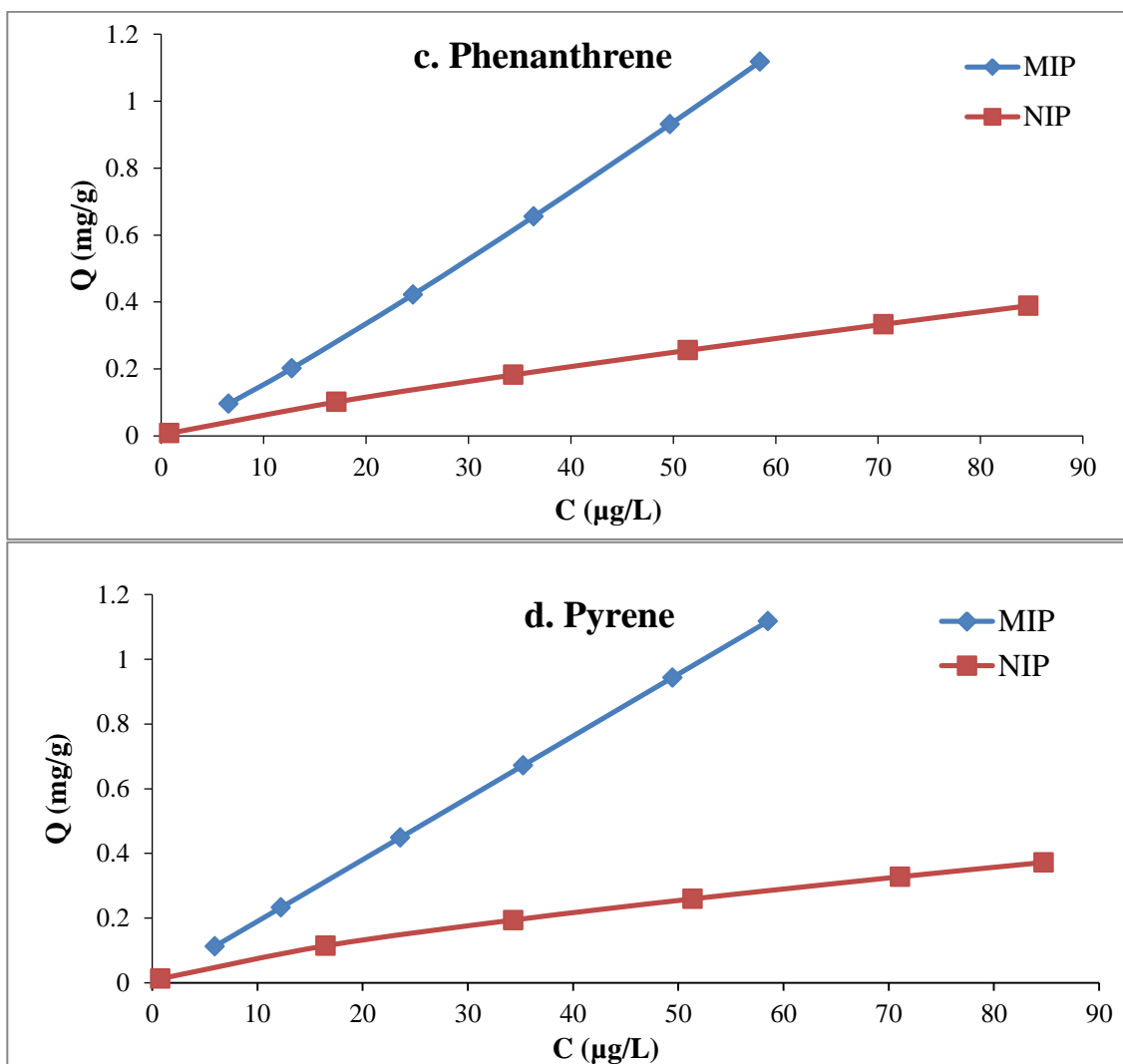


Figure 3.4(c,d) Freundlich binding isotherms graph for c) phenanthrene and d) pyrene adsorbed by for MIP/NIP uploaded in 100 mL of aqueous PAHs solution in 10-100 $\mu\text{g/L}$ concentration range.

Table 3.3 Freundlich Binding Isotherm Parameters for the Adsorption of PAHs with MIPs and NIPs

Analyte	K_f		$1/n_f$	
	MIP	NIP	MIP	NIP
Naphthalene	0.0170	0.0129	0.878	0.839
Fluorene	0.0107	0.0068	1.258	0.817
Phenanthrene	0.0115	0.0092	1.124	0.841
Pyrene	0.0189	0.0151	1.003	0.720

3.4.4. Analysis of real samples

The analytical performance of these porous MIPs (fabricated using a porogen composition chosen with a predictive model) was investigated using spiked distilled water and a real sample of produced water obtained from an oil and gas company (unnamed). Acenaphthene- d_{10} was used as the internal standard which was the same in previous experiments. The standard addition method was used to determine the concentration of PAHs in produced water in the following way: a solution of PAHs multi-standard was spiked into the produced water to make fortified concentrations of 0, 10, 30 and 50 $\mu\text{g/L}$ PAH. MIPs were placed in 100 mL of each solution with stirring for 2 h this was repeated three times for each concentration. Sets of three replicates for uptake by NIPs at the same concentrations in each matrix were also prepared. After the uptake, PAHs were extracted from the MIPs and NIPs; the extracted analytes were analyzed by GC-MS, in SIM mode. Results for these experiments are shown in Figure 3.5 (a-d) and Table 3.4. The results in

Figure 3.5 illustrate a high coefficient of linearity for all the PAHs in produced water. Both MIPs and NIPs show a good linearity behavior for uptake of PAHs; however, MIPs show higher selectivity and sensitivity than NIPs. Based on the use of standard addition methodologies, it is possible to calculate the concentrations of PAHs in the produced water, with the results presented in Table 3. The data reveals that pyrene has the highest concentration among PAHs, which is in agreement with other reports [148]. There is some lack of agreement between the MIPs and the NIPs in the analysis of produced water. This is attributed to two factors. The first is that the NIP has a lower uptake and therefore greater uncertainty in the measurement, particularly with only four points on the calibration. The second is that produced water can be quite heterogenous (a mix of aqueous dissolved phase and a small amount of dispersed oil) and so inconsistent sampling could lead to greater heterogeneity in the data. If a confidence interval at 95% was applied the two values would be considered to be the same within the margin of error. It is also positive to note that the trends in concentrations for each of the PAHs agree.

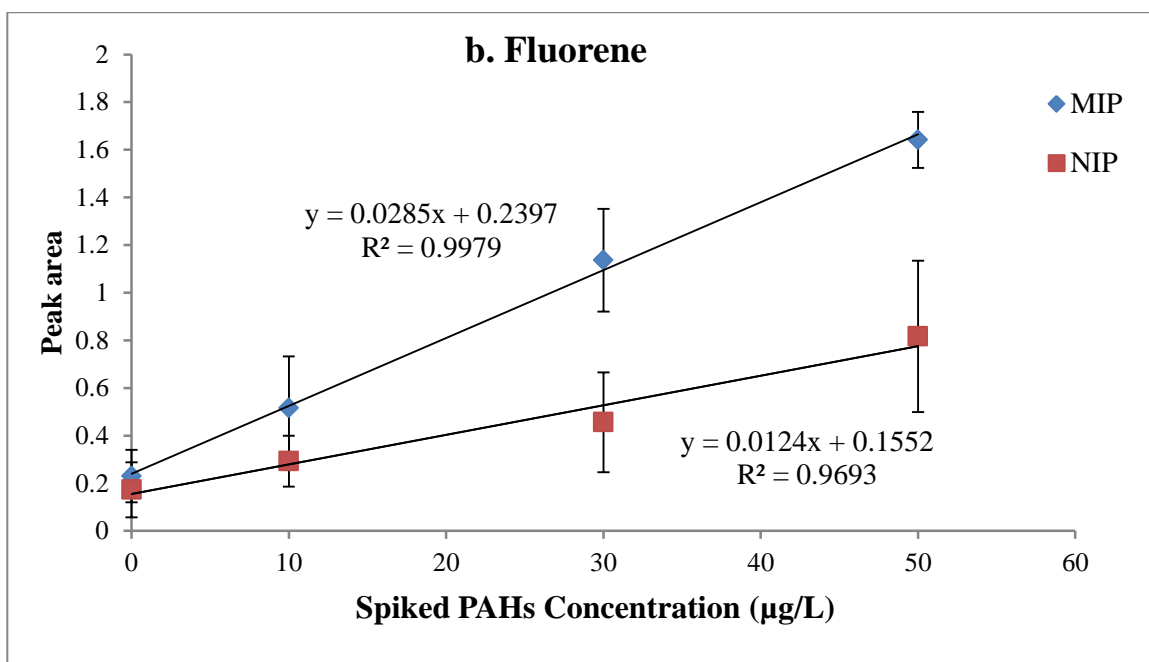
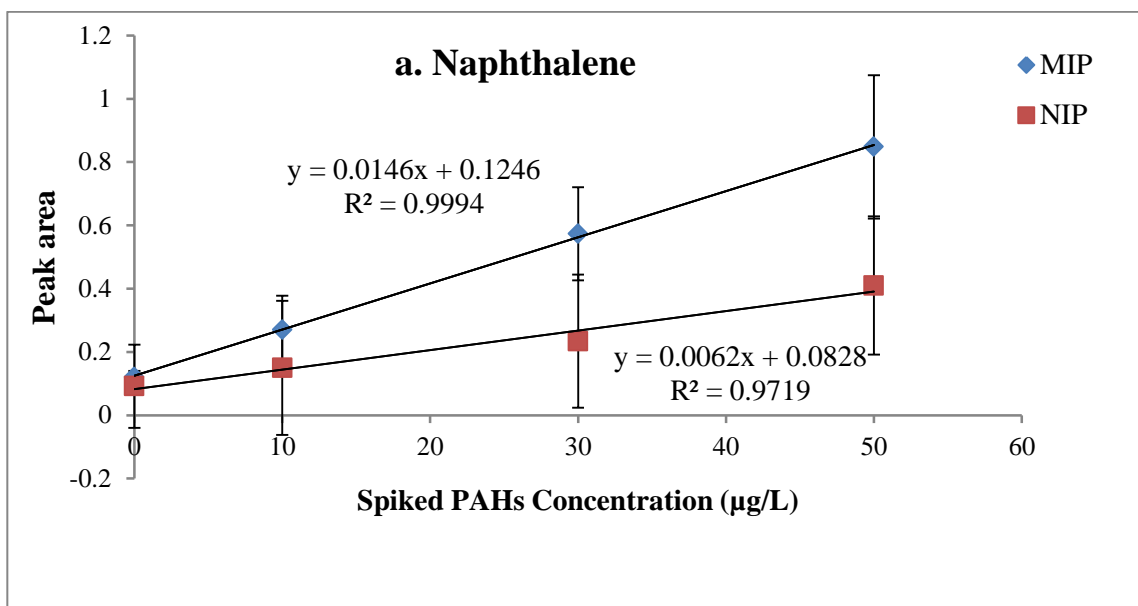


Figure 3.5(a,b) Calibration curve of a) naphthalene b) fluorene in produced water using standard addition method by GC-MS.

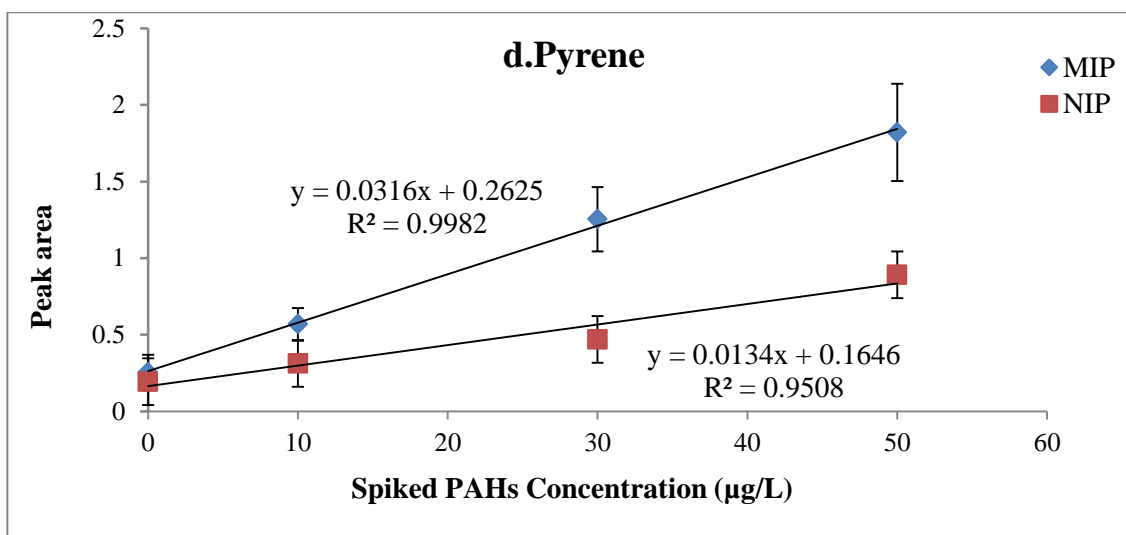
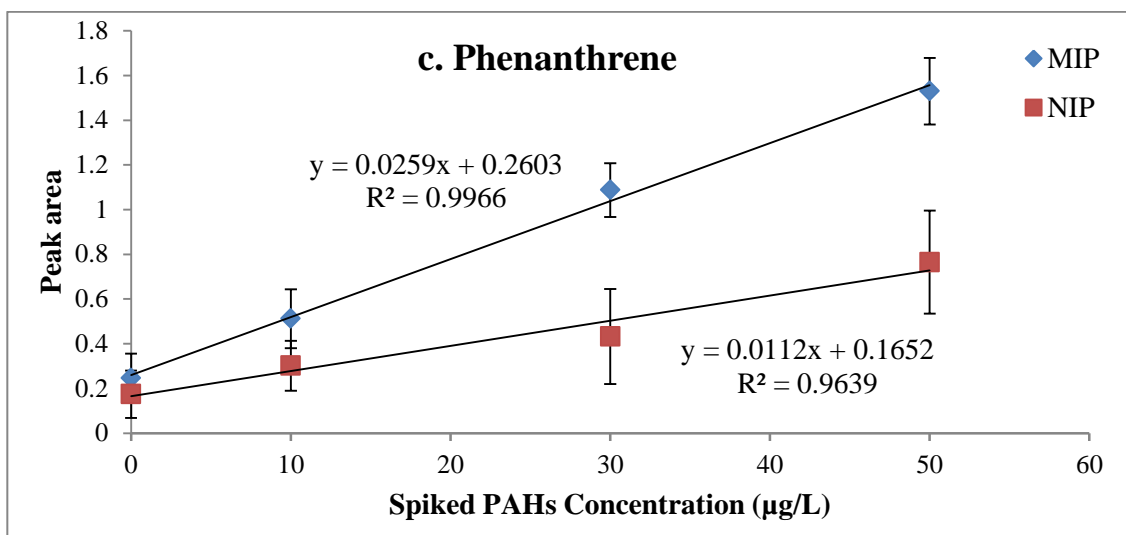


Figure 3.5(c,d) Calibration curve of c) phenanthrene d) pyrene in produced water using standard addition method by GC-MS.

Table 3.4 Concentration detected ($\mu\text{g/L}$) in produced water samples for PAHs using MIP and NIP extraction coupled to off-line GC-MS in SIM mode

PAHs	MIP	NIP
	Concentration detected \pm sd ($\mu\text{g/L}$)	Concentration detected \pm sd ($\mu\text{g/L}$)
Naphthalene	8.53 \pm 1.24	13.35 \pm 1.65
Fluorene	8.41 \pm 1.41	12.51 \pm 1.86
Phenanthrene	8.30 \pm 1.99	12.28 \pm 2.38
Pyrene	10.05 \pm 0.97	14.75 \pm 1.46

3.5 Conclusions

The results of binding studies for a series of upload and extraction experiments in aqueous multi-PAHs solutions showed that the sensitivity and affinity of MIPs is higher than NIPs. These MIPs reached equilibrium after approximately 6 h, which is considered to be a fast equilibration. In addition, analysis of the PAHs binding isotherms reveals that adsorption of PAHs by MIPs is more favorable and MIPs show higher adsorption capacity and intensity over NIPs. These porous MIPs also showed a good linearity behavior for uptake of PAHs from a real sample which was spiked produced water.

Chapter 4 Conclusions and Future Work

4.1. Conclusions

In this work, low cost, uniform, porous MIPs with high selectivity were prepared to use for detection of PAHs in water. To obtain an MIP with high analytical performance, the MIP must be highly uniform and show high porosity. This is optimized through the use of HSPs for the systematic selection of the porogenic solvent.

We prepared MIP thin-films on a derivatized glass slides as a selective sorbent and uploaded the PAHs on the thin-films followed by GC-MS analysis after extraction of the analytes (PAHs compounds) from the film by a solvent. In Chapter 2, the preparation of the MIP as a thin-film is described in detail. An innovative use of Hansen's solubility parameters was applied for selection of the optimal porogen for uniform and porous MIPs. The most uniform MIP with highest porosity was achieved by using mixed solution of 1-octanol/methanol (80: 20 v/v) as the porogenic solvent. Porosity and morphology were confirmed by SEM of the MIPs prepared with various porogens. The SEM images reveal that the MIP thin-films are highly porous with uniform shape in all parts of thin-films.

In Chapter 3, the results of the tests of selectivity and sensitivity of MIPs and NIPs for PAHs binding studies were reported for a series of upload and extraction experiments in aqueous multi-PAHs solutions. The results revealed that the affinity of MIPs is higher than NIPs, which is due to the presence of imprinted sites leading to selective binding between the target molecules and the functionalized polymer. The effect of time

on the PAHs adsorption was also studied, showing that the MIPs reached equilibrium in a short period of time (after almost 6 h). The imprinting effects of MIPs were evaluated using Freundlich fitting parameters based on analysis of the PAHs binding isotherms. The K_F (Freundlich adsorption capacity constant) and n_f (adsorption intensity) are Freundlich fitting parameters. Adsorption of PAHs by MIPs is more favorable and MIPs show higher adsorption capacity and intensity over NIPs due to the larger K_F and larger $1/n_f$ value of MIPs than NIPs.

The performance of porous MIPs fabricated using the predictive model for porogen selection was assessed using a simple distilled water sample as well as spiked produced water obtained from an oil and gas company. The results illustrated that the MIP performance was superior to the NIPs, with a higher absorption profile that was linear for all the PAHs in both types of water, distilled and produced. Both MIPs and NIPs show a good linearity behavior for uptake of PAHs; however, MIPs show higher selectivity and sensitivity than NIPs. The results for the analysis of produced water are consistent with those reported in the literature.

4.2 Future work

The use of HSPs has been shown to be a promising approach for the selection of porogenic solvents in the fabrication of MIP films. This approach solves many issues faced in the preparation of monolithic porous films, such as uniformity of thickness and porosity, which makes the performance of MIP films less reproducible and therefore has a critical effect on the applications of these sorbents.

The next step will be to study porosity and analytical performance more systematically by measuring porosity changes in materials as a consequence of solvent composition and relating that to HSPs. It is also of interest to apply this approach to a wider array of systems including new solvent systems, monomers and cross-linkers with the aim of improving the stability of the thin-films and their performance efficiency for new analytes, particularly classes of compounds that have not been targeted for MIP film development previously.

5. References

- [1] D.C. Sherrington, Preparation, structure and morphology of polymer supports, *Chemical Communications*, (1998) 2275-2286.
- [2] G.C. Vebber, P. Pranke, C.N. Pereira, Calculating Hansen solubility parameters of polymers with genetic algorithms, *Journal of Applied Polymer Science*, 131 (2014).
- [3] O. Okay, Macroporous copolymer networks, *Progress in Polymer Science*, 25 (2000) 711-779.
- [4] F. Svec, J.M. Frechet, Temperature, a simple and efficient tool for the control of pore size distribution in macroporous polymers, *Macromolecules*, 28 (1995) 7580-7582.
- [5] B.P. Santora, M.R. Gagné, K.G. Moloy, N.S. Radu, Porogen and cross-linking effects on the surface area, pore volume distribution, and morphology of macroporous polymers obtained by bulk polymerization, *Macromolecules*, 34 (2001) 658-661.
- [6] N. Topp, K. Pepper, 690. Properties of ion-exchange resins in relation to their structure. Part I. Titration curves, *Journal of the Chemical Society (Resumed)*, (1949) 3299-3303.
- [7] M. Benaglia, A. Puglisi, F. Cozzi, Polymer-supported organic catalysts, *Chemical Reviews*, 103 (2003) 3401-3430.
- [8] R. Bakry, G.K. Bonn, D. Mair, F. Svec, Monolithic porous polymer layer for the separation of peptides and proteins using thin-layer chromatography coupled with MALDI-TOF-MS, in: *Analytical Chemistry*, 2007, pp. 486-493.
- [9] H.E. Staudinger H. , One highly polymeric compounds, 116(th) Announcement On the limite swellable poly-styrene *Berichte der Deutschen Chemischen Gesellschaft*, 68 (1935) 1618.
- [10] M.R. Buchmeiser, Polymeric monolithic materials: syntheses, properties, functionalization and applications, *Polymer*, 48 (2007) 2187-2198.
- [11] E.F. Hilder, F. Svec, J.M. Frechet, Polymeric monolithic stationary phases for capillary electrochromatography, *Electrophoresis*, 23 (2002) 3934-3953.
- [12] E.P. Nesterenko, P.N. Nesterenko, D. Connolly, F. Lacroix, B. Paull, Micro-bore titanium housed polymer monoliths for reversed-phase liquid chromatography of small molecules, *Journal of Chromatography A*, 1217 (2010) 2138-2146.
- [13] H.-Y. Huang, C.-L. Lin, C.-Y. Wu, Y.-J. Cheng, C.-H. Lin, Metal organic framework–organic polymer monolith stationary phases for capillary electrochromatography and nano-liquid chromatography, *Analytica Chimica Acta*, 779 (2013) 96-103.
- [14] S. Dubinsky, H. Zhang, Z. Nie, I. Gourevich, D. Voicu, M. Deetz, E. Kumacheva, Microfluidic synthesis of macroporous copolymer particles, *Macromolecules*, 41 (2008) 3555-3561.
- [15] A.I. Cooper, C.D. Wood, A.B. Holmes, Synthesis of well-defined macroporous polymer monoliths by sol– gel polymerization in supercritical CO₂, *Industrial & Engineering Chemistry Research*, 39 (2000) 4741-4744.
- [16] E.C. Peters, F. Svec, J.M. Frechet, Rigid macroporous polymer monoliths, *Advanced Materials*, 11 (1999) 1169-1181.

- [17] M.J. Beneš, D. Horák, F. Svec, Methacrylate-based chromatographic media, *Journal of Separation Science*, 28 (2005) 1855-1875.
- [18] J. Lee, D.R. Hwang, S.E. Shim, Y.-M. Rhym, Controlling morphology of polymer microspheres by Shirasu porous glass (SPG) membrane emulsification and subsequent polymerization: from solid to hollow, *Macromolecular Research*, 18 (2010) 1142-1147.
- [19] C. Cheng, J. Vanderhoff, M. El-Aasser, Monodisperse porous polymer particles: formation of the porous structure, *Journal of Polymer Science Part A: Polymer Chemistry*, 30 (1992) 245-256.
- [20] J. Ugelstad, H. Mfutakamba, P. Mørk, T. Ellingsen, A. Berge, R. Schmid, L. Holm, A. Jørgedal, F. Hansen, K. Nustad, Preparation and application of monodisperse polymer particles, in: *Journal of Polymer Science: Polymer Symposia*, Wiley Online Library, 1985, pp. 225-240.
- [21] C. Cheng, F. Micale, J. Vanderhoff, M. El-Aasser, Synthesis and characterization of monodisperse porous polymer particles, *Journal of Polymer Science Part A: Polymer Chemistry*, 30 (1992) 235-244.
- [22] F. Svec, J.M. Fréchet, Continuous rods of macroporous polymer as high-performance liquid chromatography separation media, *Analytical Chemistry*, 64 (1992) 820-822.
- [23] S. Xie, R. Allington, J. Fréchet, F. Svec, Porous polymer monoliths: an alternative to classical beads, *Modern Advances in Chromatography*, (2002) 87-125.
- [24] J. Ortiz-Palacios, J. Cardoso, O. Manero, Production of macroporous resins for heavy-metal removal. I. Nonfunctionalized polymers, *Journal of Applied Polymer Science*, 107 (2008) 2203-2210.
- [25] F.S. Macintyre, D.C. Sherrington, Control of porous morphology in suspension polymerized poly (divinylbenzene) resins using oligomeric porogens, *Macromolecules*, 37 (2004) 7628-7636.
- [26] M. Hamid, R. Naheed, M. Fuzail, E. Rehman, The effect of different diluents on the formation of N-vinylcarbazole-divinylbenzene copolymer beads, *European Polymer Journal*, 35 (1999) 1799-1811.
- [27] D. Rabelo, F. Coutinho, Structure and properties of styrene-divinylbenzene copolymers, *Polymer Bulletin*, 33 (1994) 479-486.
- [28] M.H. Mohamed, L.D. Wilson, Porous copolymer resins: Tuning pore structure and surface area with non reactive porogens, *Nanomaterials*, 2 (2012) 163-186.
- [29] C. Yu, F. Svec, J.M. Frechet, Towards stationary phases for chromatography on a microchip: molded porous polymer monoliths prepared in capillaries by photoinitiated in situ polymerization as separation media for electrochromatography, *Electrophoresis*, 21 (2000) 120-127.
- [30] A. Sarafraz-Yazdi, N. Razavi, Application of molecularly-imprinted polymers in solid-phase microextraction techniques, *TrAC Trends in Analytical Chemistry*, 73 (2015) 81-90.
- [31] S. Yu, F.L. Ng, K.C.C. Ma, A.A. Mon, F.L. Ng, Y.Y. Ng, Effect of porogenic solvent on the porous properties of polymer monoliths, *Journal of Applied Polymer Science*, 127 (2013) 2641-2647.

- [32] K. Dušek, Phase separation during the formation of three-dimensional polymers, in: *Journal of Polymer Science: Polymer Symposia*, 1967, pp. 1289-1299.
- [33] C.M. Hansen, 50 Years with solubility parameters—past and future, *Progress in Organic Coatings*, 51 (2004) 77-84.
- [34] C.M. Hansen, The three dimensional solubility parameter, Danish Technical: Copenhagen, (1967) 14.
- [35] C.A. Lipinski, F. Lombardo, B.W. Dominy, P.J. Feeney, Experimental and computational approaches to estimate solubility and permeability in drug discovery and development settings, *Advanced Drug Delivery Reviews*, 64 (2012) 4-17.
- [36] S. Scheler, A novel approach to the interpretation and prediction of solvent effects in the synthesis of macroporous polymers, *Journal of Applied Polymer Science*, 105 (2007) 3121-3131.
- [37] E. Benito-Peña, F. Navarro-Villoslada, S. Carrasco, S. Jockusch, M.F. Ottaviani, M.C. Moreno-Bondi, Experimental mixture design as a tool for the synthesis of antimicrobial selective molecularly imprinted monodisperse microbeads, *ACS Applied Materials & Interfaces*, 7 (2015) 10966-10976.
- [38] M.L. Huggins, The Solubility of Nonelectrolytes. By Joel H. Hildebrand and Robert S. Scott, *The Journal of Physical Chemistry*, 55 (1951) 619-620.
- [39] A.F. Barton, *Handbook of polymer-liquid interaction parameters and solubility parameters*, CRC press, 1990.
- [40] J. Brandrup, E.H. Immergut, E.A. Grulke, A. Abe, D.R. Bloch, *Polymer handbook*, Wiley New York etc, 1989.
- [41] J.H. Hildebrand, A critique of the theory of solubility of non-electrolytes, *Chemical Reviews*, 44 (1949) 37-45.
- [42] E.C. Goh, H.D. Stöver, Cross-Linked Poly (methacrylic acid-co-poly (ethylene oxide) methyl ether methacrylate) Microspheres and Microgels Prepared by Precipitation Polymerization: A Morphology Study, *Macromolecules*, 35 (2002) 9983-9989.
- [43] H.W. Milliman, D. Boris, D.A. Schiraldi, Experimental determination of Hansen solubility parameters for select POSS and polymer compounds as a guide to POSS–polymer interaction potentials, *Macromolecules*, 45 (2012) 1931-1936.
- [44] O. Fuchs, *The Molecular Theory of Solutions*. Von I. Prigogine, A. Bellemans und V. Mathot. North-Holland Publishing Company, Amsterdam 1957. 1. Aufl., XX, 448 S., 120 Abb., geb. Hfl. 48.-, *Angewandte Chemie*, 70 (1958) 613-613.
- [45] M. Levin, P. Redelius, Determining the Hansen solubility parameter of three corrosion inhibitors and the correlation with mineral oil, *Energy & Fuels*, 26 (2012) 7243-7250.
- [46] F. Gharagheizi, M. Torabi Angaji, A new improved method for estimating Hansen solubility parameters of polymers, *Journal of Macromolecular Science, Part B: Physics*, 45 (2006) 285-290.
- [47] J. Ma, L. Zhou, A new procedure for calculating Hansen solubility parameters of carbon nanotube/polymer composites, *Polymer Bulletin*, 68 (2012) 1053-1063.
- [48] G. Wulff, T. Gross, R. Schönfeld, Enzyme models based on molecularly imprinted polymers with strong esterase activity, *Angewandte Chemie International Edition*, 36 (1997) 1962-1964.

- [49] T. Takeuchi, J. Matsui, Molecular imprinting: An approach to “tailor-made” synthetic polymers with biomimetic functions, *Acta Polymerica*, 47 (1996) 471-480.
- [50] D. Kriz, O. Ramström, K. Mosbach, Peer reviewed: molecular imprinting: New possibilities for sensor technology, *Analytical Chemistry*, 69 (1997) 345A-349A.
- [51] V.T. Remcho, Z.J. Tan, Peer Reviewed: MIPs as Chromatographic Stationary Phases for Molecular Recognition, *Analytical Chemistry*, 71 (1999) 248A-255A.
- [52] C. Alexander, L. Davidson, W. Hayes, Imprinted polymers: artificial molecular recognition materials with applications in synthesis and catalysis, *Tetrahedron*, 59 (2003) 2025-2057.
- [53] E. Caro, R.M. Marcé, P.A. Cormack, D.C. Sherrington, F. Borrull, On-line solid-phase extraction with molecularly imprinted polymers to selectively extract substituted 4-chlorophenols and 4-nitrophenol from water, *Journal of Chromatography A*, 995 (2003) 233-238.
- [54] T. Kitade, K. Kitamura, T. Konishi, S. Takegami, T. Okuno, M. Ishikawa, M. Wakabayashi, K. Nishikawa, Y. Muramatsu, Potentiometric immunosensor using artificial antibody based on molecularly imprinted polymers, *Analytical Chemistry*, 76 (2004) 6802-6807.
- [55] K. Haupt, Peer reviewed: molecularly imprinted polymers: the next generation, in, ACS Publications, 2003.
- [56] X. Shen, L. Ye, Molecular imprinting in Pickering emulsions: a new insight into molecular recognition in water, *Chemical Communications*, 47 (2011) 10359-10361.
- [57] X. Luo, F. Deng, S. Luo, X. Tu, L. Yang, Grafting of molecularly imprinted polymers from the surface of Fe₃O₄ nanoparticles containing double bond via suspension polymerization in aqueous environment: A selective sorbent for theophylline, *Journal of Applied Polymer Science*, 121 (2011) 1930-1937.
- [58] E.L. Berkeley, Porous polymer monoliths: simple and efficient mixers prepared by direct polymerization in the channels of microfluidic chips, *Electrophoresis*, 22 (2001) 3959-3967.
- [59] D.A. Olson, L. Chen, M.A. Hillmyer, Templating nanoporous polymers with ordered block copolymers, *Chemistry of Materials*, 20 (2007) 869-890.
- [60] X. Hu, Q. An, G. Li, S. Tao, J. Liu, Imprinted photonic polymers for chiral recognition, *Angewandte Chemie International Edition*, 45 (2006) 8145-8148.
- [61] S.N. Egli, E.D. Butler, C.S. Bottaro, Selective extraction of light polycyclic aromatic hydrocarbons in environmental water samples with pseudo-template thin-film molecularly imprinted polymers, *Analytical Methods*, 7 (2015) 2028-2035.
- [62] T. Piacham, Å. Josell, H. Arwin, V. Prachayasittikul, L. Ye, Molecularly imprinted polymer thin films on quartz crystal microbalance using a surface bound photo-radical initiator, *Analytica Chimica Acta*, 536 (2005) 191-196.
- [63] L. Chen, X. Wang, W. Lu, X. Wu, J. Li, Molecular imprinting: perspectives and applications, *Chemical Society Reviews*, 45 (2016) 2137-2211.
- [64] E.N. Ndunda, B. Mizaikoff, Molecularly imprinted polymers for the analysis and removal of polychlorinated aromatic compounds in the environment: a review, *Analyst*, 141 (2016) 3141-3156.
- [65] D.A. Spivak, Optimization, evaluation, and characterization of molecularly imprinted polymers, *Advanced Drug Delivery Reviews*, 57 (2005) 1779-1794.

- [66] P.A. Cormack, A.Z. Elorza, Molecularly imprinted polymers: synthesis and characterisation, *Journal of Chromatography B*, 804 (2004) 173-182.
- [67] L.I. Andersson, I.A. Nicholls, K. Mosbach, Molecular imprinting: the current status and future development of polymer-based recognition systems, *Advances in molecular and cell biology*, 15 (1996) 651-670.
- [68] D. Kriz, R. Ansell, Man Made Mimics of Antibodies and their Application in Analytical Chemistry, *Molecularly Imprinted Polymers*, 23 (2001) 417-436.
- [69] E. Yilmaz, K. Mosbach, K. Haupt, Influence of functional and cross-linking monomers and the amount of template on the performance of molecularly imprinted polymers in binding assays, *Analytical Communications*, 36 (1999) 167-170.
- [70] H. Kim, D.A. Spivak, New insight into modeling non-covalently imprinted polymers, *Journal of the American Chemical Society*, 125 (2003) 11269-11275.
- [71] H.-Y. Lin, C.-Y. Hsu, J.L. Thomas, S.-E. Wang, H.-C. Chen, T.-C. Chou, The microcontact imprinting of proteins: The effect of cross-linking monomers for lysozyme, ribonuclease A and myoglobin, *Biosensors and Bioelectronics*, 22 (2006) 534-543.
- [72] Y. Zhang, D. Song, L.M. Lanni, K.D. Shimizu, Importance of functional monomer dimerization in the molecular imprinting process, *Macromolecules*, 43 (2010) 6284-6294.
- [73] H. Yan, K.H. Row, Characteristic and synthetic approach of molecularly imprinted polymer, *International Journal of Molecular Sciences*, 7 (2006) 155-178.
- [74] M. Kempe, K. Mosbach, Molecular imprinting used for chiral separations, *Journal of Chromatography A*, 694 (1995) 3-13.
- [75] C. Sulitzky, B. Rückert, A.J. Hall, F. Lanza, K. Unger, B. Sellergren, Grafting of molecularly imprinted polymer films on silica supports containing surface-bound free radical initiators, *Macromolecules*, 35 (2002) 79-91.
- [76] W.K. Busfield, I.D. Jenkins, P. Van Le, Investigations into the AIBN initiation steps in the free radical polymerisation of acrylonitrile by the aminoxyl trapping technique, *Polymer Bulletin*, 36 (1996) 435-441.
- [77] P. Wang, X. Sun, X. Su, T. Wang, Advancements of molecularly imprinted polymers in the food safety field, *Analyst*, 141 (2016) 3540-3553.
- [78] G. Wulff, S. Schauhoff, Enzyme-analog-built polymers. 27. Racemic resolution of free sugars with macroporous polymers prepared by molecular imprinting. Selectivity dependence on the arrangement of functional groups versus spatial requirements, *The Journal of Organic Chemistry*, 56 (1991) 395-400.
- [79] G. Wulff, A. Sarhan, K. Zabrocki, Enzyme-analogue built polymers and their use for the resolution of racemates, *Tetrahedron Letters*, 14 (1973) 4329-4332.
- [80] A. Bossi, F. Bonini, A. Turner, S. Piletsky, Molecularly imprinted polymers for the recognition of proteins: the state of the art, *Biosensors and Bioelectronics*, 22 (2007) 1131-1137.
- [81] L. Andersson, B. Sellergren, K. Mosbach, Imprinting of amino acid derivatives in macroporous polymers, *Tetrahedron Letters*, 25 (1984) 5211-5214.
- [82] B. Sellergren, A.J. Hall, Molecularly imprinted polymers as antibody mimics in automated on-line fluorescent competitive assays, *Analytical chemistry*, 13 (2007) 4915-4923.

- [83] L.I. Andersson, Molecular imprinting: developments and applications in the analytical chemistry field, *Journal of Chromatography B: Biomedical Sciences and Applications*, 745 (2000) 3-13.
- [84] B. Sellergren, Noncovalent molecular imprinting: antibody-like molecular recognition in polymeric network materials, *TrAC Trends in Analytical Chemistry*, 16 (1997) 310-320.
- [85] A. Mayes, M. Whitcombe, Synthetic strategies for the generation of molecularly imprinted organic polymers, *Advanced Drug Delivery Reviews*, 57 (2005) 1742-1778.
- [86] E.E. Stashenko, B.E. Jaramillo, J.R. Martínez, Comparison of different extraction methods for the analysis of volatile secondary metabolites of *Lippia alba* (Mill.) NE Brown, grown in Colombia, and evaluation of its in vitro antioxidant activity, *Journal of Chromatography A*, 1025 (2004) 93-103.
- [87] D.C. Harris, *Quantitative chemical analysis*, Macmillan, 2010.
- [88] H.-J. Hübschmann, *Handbook of GC-MS: Fundamentals and applications*, John Wiley & Sons, 2015.
- [89] C.H. Hartmann, Gas chromatography detectors, *Analytical Chemistry*, 43 (1971) 113-125.
- [90] A.E. Ashcroft, *Ionization methods in organic mass spectrometry*, Royal Society of Chemistry, 2007.
- [91] P. Tibbetts, I. Buchanan, L. Gawel, R. Large, A comprehensive determination of produced water composition, in: *Produced Water*, Springer, 1992, pp. 97-112.
- [92] J. Neff, K. Lee, E.M. DeBlois, Produced water: overview of composition, fates, and effects, in: *Produced water*, Springer, 2011, pp. 3-54.
- [93] R. Jacobs, R. Grant, J. Kwant, J. Marquenie, E. Mentzer, The composition of produced water from Shell operated oil and gas production in the North Sea, in: *Produced Water*, Springer, 1992, pp. 13-21.
- [94] D.A. Pillard, J.E. Tietge, J.M. Evans, Estimating the acute toxicity of produced waters to marine organisms using predictive toxicity models, *Produced Water 2: Environmental Issues and Mitigation Technologies*, (1996) 49.
- [95] K.B. Gregory, R.D. Vidic, D.A. Dzombak, Water management challenges associated with the production of shale gas by hydraulic fracturing, *Elements*, 7 (2011) 181-186.
- [96] L.-G. Faksness, P.G. Grini, P.S. Daling, Partitioning of semi-soluble organic compounds between the water phase and oil droplets in produced water, *Marine Pollution Bulletin*, 48 (2004) 731-742.
- [97] G. Terrens, R. Tait, Monitoring ocean concentrations of aromatic hydrocarbons from produced formation water discharges to Bass Strait, Australia, in: *SPE Health, Safety and Environment in Oil and Gas Exploration and Production Conference*, Society of Petroleum Engineers, 1996.
- [98] J.M. Neff, S. Johnsen, T.K. Frost, T.I.R. Utvik, G.S. Durell, Oil well produced water discharges to the North Sea. Part II: comparison of deployed mussels (*Mytilus edulis*) and the DREAM model to predict ecological risk, *Marine Environmental Research*, 62 (2006) 224-246.
- [99] J.A. Veil, Comparison of two international approaches to controlling risk from produced water discharges, in: *70th PERF meeting*, Paris, France, 2006.

- [100] G. Fraser, J. Ellis, L. Hussain, An international comparison of governmental disclosure of hydrocarbon spills from offshore oil and gas installations, *Marine Pollution Bulletin*, 56 (2008) 9-13.
- [101] E. Manoli, C. Samara, Polycyclic aromatic hydrocarbons in natural waters: sources, occurrence and analysis, *TrAC Trends in Analytical Chemistry*, 18 (1999) 417-428.
- [102] H.K. Bojes, P.G. Pope, Characterization of EPA's 16 priority pollutant polycyclic aromatic hydrocarbons (PAHs) in tank bottom solids and associated contaminated soils at oil exploration and production sites in Texas, *Regulatory Toxicology and Pharmacology*, 47 (2007) 288-295.
- [103] R.J. Law, J.L. Biscaya, Polycyclic aromatic hydrocarbons (PAH)—problems and progress in sampling, analysis and interpretation, *Marine Pollution Bulletin*, 29 (1994) 235-241.
- [104] R.J. Krupadam, M.S. Khan, S.R. Wate, Removal of probable human carcinogenic polycyclic aromatic hydrocarbons from contaminated water using molecularly imprinted polymer, *Water Research*, 44 (2010) 681-688.
- [105] A. Rubio-Clemente, R.A. Torres-Palma, G.A. Peñuela, Removal of polycyclic aromatic hydrocarbons in aqueous environment by chemical treatments: a review, *Science of the Total Environment*, 478 (2014) 201-225.
- [106] A.L.C. Lima, T.I. Eglinton, C.M. Reddy, High-resolution record of pyrogenic polycyclic aromatic hydrocarbon deposition during the 20th century, *Environmental Science & Technology*, 37 (2003) 53-61.
- [107] J. de Boer, R.J. Law, Developments in the use of chromatographic techniques in marine laboratories for the determination of halogenated contaminants and polycyclic aromatic hydrocarbons, *Journal of Chromatography A*, 1000 (2003) 223-251.
- [108] R. Yang, N. Zhao, X. Xiao, S. Yu, J. Liu, W. Liu, Determination of Polycyclic Aromatic Hydrocarbons in the Presence of Humic Acid in water, *Applied Spectroscopy*, 70 (2016) 1520-1528.
- [109] P. Roose, A.T. Udo, Monitoring organic microcontaminants in the marine environment: principles, programmes and progress, *TrAC Trends in Analytical Chemistry*, 24 (2005) 897-926.
- [110] J. Arey, Atmospheric reactions of PAHs including formation of nitroarenes, in: *PAHs and related compounds*, Springer, 1998, pp. 347-385.
- [111] D.L. Poster, M.M. Schantz, L.C. Sander, S.A. Wise, Analysis of polycyclic aromatic hydrocarbons (PAHs) in environmental samples: a critical review of gas chromatographic (GC) methods, *Analytical and Bioanalytical Chemistry*, 386 (2006) 859-881.
- [112] U.E.P. Agency, Methods for the determination of organic compounds in drinking water supplement, I, EPA/600/4-90/020, National Technical Information Service, PB91-146027, Washington D.C, (1990).
- [113] US Environmental Protection Agency Methods for the determination of organic compounds in drinking water-supplement III, EPA/600/R-95-131, National Technical Information Service, PB95-261616, Washington D.C., (1995).
- [114] US Environmental Protection Agency, Determination of polynuclear aromatic hydrocarbons in industrial and municipal wastewaters, EPA 600/4-82-025, National Technical Information Service, PB82-258799, Springfield, VA, , (1982).

- [115] US Environmental Protection Agency, Method 625-base/ neutrals and acids, PART 136 methods for organic chemical analysis of municipal and industrial wastewater, 40CFR136.1, US Environmental Protection Agency, Washington D.C., (2005).
- [116] US Environmental Protection Agency, Method 610- polynuclear aromatic hydrocarbons, PART 136 guidelines establishing test procedures for the analysis of pollutants; appendix A: methods for organic chemical analysis of municipal and industrial wastewater, 40CFR136.1, US Environmental Protection Agency, Washington D.C., (2005).
- [117] C. Yan, R. Dadoo, H. Zhao, R.N. Zare, D.J. Rakestraw, Capillary electrochromatography: analysis of polycyclic aromatic hydrocarbons, *Analytical Chemistry*, 67 (1995) 2026-2029.
- [118] H. Sharma, V. Jain, Z.H. Khan, Identification of polycyclic aromatic hydrocarbons (PAHs) in suspended particulate matter by synchronous fluorescence spectroscopic technique, *Spectrochimica Acta Part A: Molecular and Biomolecular Spectroscopy*, 68 (2007) 43-49.
- [119] S.A. Wise, L.R. Hilpert, G.D. Byrd, W.E. May, Comparison of liquid chromatography with fluorescence detection and gas chromatography/mass spectrometry for the determination of polycyclic aromatic hydrocarbons in environmental samples, *Polycyclic Aromatic Compounds*, 1 (1990) 81-98.
- [120] A. Christensen, C. Östman, R. Westerholm, Ultrasound-assisted extraction and on-line LC–GC–MS for determination of polycyclic aromatic hydrocarbons (PAH) in urban dust and diesel particulate matter, *Analytical and Bioanalytical Chemistry*, 381 (2005) 1206-1216.
- [121] T. Kubo, S. Arimura, Y. Tominaga, T. Naito, K. Hosoya, K. Otsuka, Molecularly imprinted polymers for selective adsorption of lysozyme and cytochrome c using a PEG-based hydrogel: selective recognition for different conformations due to pH conditions, *Macromolecules*, 48 (2015) 4081-4087.
- [122] M.C. Moreno-Bondi, F. Navarro-Villoslada, E. Benito-Peña, J.L. Urraca, Molecularly imprinted polymers as selective recognition elements in optical sensing, *Current Analytical Chemistry*, 4 (2008) 316-340.
- [123] S.A. Piletsky, H. Matuschewski, U. Schedler, A. Wilpert, E.V. Piletska, T.A. Thiele, M. Ulbricht, Surface functionalization of porous polypropylene membranes with molecularly imprinted polymers by photograft copolymerization in water, *Macromolecules*, 33 (2000) 3092-3098.
- [124] L. Wu, K. Zhu, M. Zhao, Y. Li, Theoretical and experimental study of nicotinamide molecularly imprinted polymers with different porogens, *Analytica Chimica Acta*, 549 (2005) 39-44.
- [125] R.J. Ansell, K. Mosbach, Molecularly imprinted polymers by suspension polymerisation in perfluorocarbon liquids, with emphasis on the influence of the porogenic solvent, *Journal of Chromatography A*, 787 (1997) 55-66.
- [126] A. Sariban, K. Binder, Phase separation of polymer mixtures in the presence of solvent, *Macromolecules*, 21 (1988) 711-726.
- [127] A. Barbetta, N.R. Cameron, Morphology and surface area of emulsion-derived (PolyHIPE) solid foams prepared with oil-phase soluble porogenic solvents: Three-component surfactant system, *Macromolecules*, 37 (2004) 3202-3213.

- [128] C. Luo, M. Nangrejo, M. Edirisinghe, A novel method of selecting solvents for polymer electrospinning, *Polymer*, 51 (2010) 1654-1662.
- [129] J. Lara, F. Zimmermann, D. Drolet, C.M. Hansen, A. Chollot, N. Monta, The use of the Hansen solubility parameters in the selection of protective polymeric materials resistant to chemicals, *International Journal of Current Research*, 9 (2017) 47860-47867.
- [130] C.M. Hansen, Hansen solubility parameters: a user's handbook, CRC press, 2007.
- [131] M. Terada, R. Marchessault, Determination of solubility parameters for poly (3-hydroxyalkanoates), *International Journal of Biological Macromolecules*, 25 (1999) 207-215.
- [132] Y.V. Pashin, L. Bakhitova, Mutagenic and carcinogenic properties of polycyclic aromatic hydrocarbons, *Environmental Health Perspectives*, 30 (1979) 185.
- [133] G. Cornelissen, S.E. Hale, 11 Polycyclic aromatic hydrocarbons in biochar, *Biochar: A Guide to Analytical Methods*, (2017) 126.
- [134] C. Muangchinda, A. Yamazoe, D. Polrit, H. Thoetkiattikul, W. Mhuanong, V. Champreda, O. Pinyakong, Biodegradation of high concentrations of mixed polycyclic aromatic hydrocarbons by indigenous bacteria from a river sediment: a microcosm study and bacterial community analysis, *Environmental Science and Pollution Research*, 24 (2017) 4591-4602.
- [135] R.A. Omores, F. Wewers, P.O. Ikhide, T. Farrar, A.-r. Giwa, Spatio-Temporal Distribution of Polycyclic Aromatic Hydrocarbons in Urban Soils in Cape Town, South Africa, *International Journal of Environmental Research*, (2017) 1-8.
- [136] E. Fasano, I. Yebra-Pimentel, E. Martínez-Carballo, J. Simal-Gándara, Profiling, distribution and levels of carcinogenic polycyclic aromatic hydrocarbons in traditional smoked plant and animal foods, *Food Control*, 59 (2016) 581-590.
- [137] S.A. da Silva, G.R. Sampaio, E.A.F. da Silva Torres, Optimization and validation of a method using UHPLC-fluorescence for the analysis of polycyclic aromatic hydrocarbons in cold-pressed vegetable oils, *Food Chemistry*, 221 (2017) 809-814.
- [138] M. Chen, P. Xu, G. Zeng, C. Yang, D. Huang, J. Zhang, Bioremediation of soils contaminated with polycyclic aromatic hydrocarbons, petroleum, pesticides, chlorophenols and heavy metals by composting: applications, microbes and future research needs, *Biotechnology Advances*, 33 (2015) 745-755.
- [139] B.S. Peterson, V.A. Rauh, R. Bansal, X. Hao, Z. Toth, G. Nati, K. Walsh, R.L. Miller, F. Arias, D. Semanek, Effects of prenatal exposure to air pollutants (polycyclic aromatic hydrocarbons) on the development of brain white matter, cognition, and behavior in later childhood, *JAMA psychiatry*, 72 (2015) 531-540.
- [140] X.-T. Wang, Y. Miao, Y. Zhang, Y.-C. Li, M.-H. Wu, G. Yu, Polycyclic aromatic hydrocarbons (PAHs) in urban soils of the megacity Shanghai: occurrence, source apportionment and potential human health risk, *Science of the Total Environment*, 447 (2013) 80-89.
- [141] K.-H. Kim, S.A. Jahan, E. Kabir, R.J. Brown, A review of airborne polycyclic aromatic hydrocarbons (PAHs) and their human health effects, *Environment international*, 60 (2013) 71-80.
- [142] L.G. Tidwell, S.E. Allan, S.G. O'Connell, K.A. Hobbie, B.W. Smith, K.A. Anderson, Polycyclic aromatic hydrocarbon (PAH) and oxygenated PAH (OPAH) air-

water exchange during the deepwater horizon oil spill, *Environmental Science & Technology*, 49 (2015) 141.

[143] B.D.B. Tiu, R.J. Krupadam, R.C. Advincula, Pyrene-imprinted polythiophene sensors for detection of polycyclic aromatic hydrocarbons, *Sensors and Actuators B: Chemical*, 228 (2016) 693-701.

[144] P.A. Lieberzeit, F.L. Dickert, Chemosensors in environmental monitoring: challenges in ruggedness and selectivity, *Analytical and Bioanalytical Chemistry*, 393 (2009) 467.

[145] N. Pérez-Moral, A. Mayes, Comparative study of imprinted polymer particles prepared by different polymerisation methods, *Analytica Chimica Acta*, 504 (2004) 15-21.

[146] X. Shen, C. Xu, L. Ye, Molecularly imprinted polymers for clean water: Analysis and purification, *Ind. Eng. Chem. Res*, 52 (2013) 13890-13899.

[147] R.J. Umpleby, S.C. Baxter, M. Bode, J.K. Berch, R.N. Shah, K.D. Shimizu, Application of the Freundlich adsorption isotherm in the characterization of molecularly imprinted polymers, *Analytica Chimica Acta*, 435 (2001) 35-42.

[148] J.-P. Lai, R. Niessner, D. Knopp, Benzo [a] pyrene imprinted polymers: synthesis, characterization and SPE application in water and coffee samples, *Analytica Chimica Acta*, 522 (2004) 137-144.

[149] R.N. Liang, D.A. Song, R.M. Zhang, W. Qin, Potentiometric Sensing of Neutral Species Based on a Uniform-Sized Molecularly Imprinted Polymer as a Receptor, *Angewandte Chemie International Edition*, 49 (2010) 2556-2559.

[150] X. Song, J. Li, S. Xu, R. Ying, J. Ma, C. Liao, D. Liu, J. Yu, L. Chen, Determination of 16 polycyclic aromatic hydrocarbons in seawater using molecularly imprinted solid-phase extraction coupled with gas chromatography-mass spectrometry, *Talanta*, 99 (2012) 75-82.

[151] X. Song, J. Li, J. Wang, L. Chen, Quercetin molecularly imprinted polymers: Preparation, recognition characteristics and properties as sorbent for solid-phase extraction, *Talanta*, 80 (2009) 694-702.

[152] K. Foo, B. Hameed, Insights into the modeling of adsorption isotherm systems, *Chemical Engineering Journal*, 156 (2010) 2-10.

[153] R. Crisafulli, M.A.L. Milhome, R.M. Cavalcante, E.R. Silveira, D. De Keukeleire, R.F. Nascimento, Removal of some polycyclic aromatic hydrocarbons from petrochemical wastewater using low-cost adsorbents of natural origin, *Bioresource Technology*, 99 (2008) 4515-4519.

Appendix A.

MATLAB code for Target molecule's HSPs calculation

```
%%%%%%%%%%%%%%%%%%%%%%%%%%%%%%%%%%%%%%%%%%%%%%%%%%%%%%%%%%%%%%%%%%%%%%%%%
```

```
%%%%%%%%%%%%%%%%%%%%%%%%%%%%%%%%%%%%%%%%%%%%%%%%%%%%%%%%%%%%%%%%%%%%%%%%%
```

```
%%%%%%%%%%%%%%%%%%%%%%%%%%%%%%%%%%%%%%%%%%%%%%%%%%%%%%%%%%%%%%%%%%%%%%%%%
```

```
%%%%%%%%%%%%%%%%%%%%%%%%%%%%%%%%%%%%%%%%%%%%%%%%%%%%%%%%%%%%%%%%%%%%%%%%%
```

```
%%%%%%%%%%%%%%%%%%%%%%%%%%%%%%%%%%%%%%%%%%%%%%%%%%%%%%%%%%%%%%%%%%%%%%%%%
```

Target's HSPs estimations

```
%%%%%%%%%%%%%%%%%%%%%%%%%%%%%%%%%%%%%%%%%%%%%%%%%%%%%%%%%%%%%%%%%%%%%%%%%
```

```
%%%%%%%%%%%%%%%%%%%%%%%%%%%%%%%%%%%%%%%%%%%%%%%%%%%%%%%%%%%%%%%%%%%%%%%%%
```

```
%%%%%%%%%%%%%%%%%%%%%%%%%%%%%%%%%%%%%%%%%%%%%%%%%%%%%%%%%%%%%%%%%%%%%%%%%
```

```
%%%%%%%%%%%%%%%%%%%%%%%%%%%%%%%%%%%%%%%%%%%%%%%%%%%%%%%%%%%%%%%%%%%%%%%%%
```

```
%%%%%%%%%%%%%%%%%%%%%%%%%%%%%%%%%%%%%%%%%%%%%%%%%%%%%%%%%%%%%%%%%%%%%%%%%
```

```
clc
```

```
clear all
```

```
Solvent_Data;
```

```
delta_d=(data(:,1))';
```

```
delta_p=(data(:,2))';
```

```
delta_h=(data(:,3))';
```

```
solubility=(data(:,4))';
```



```

a(1)=mean(delta_d);

a(2)=mean(delta_p);

a(3)=mean(delta_h);

a(4)=sqrt(a(1)^2+a(2)^2+a(3)^2);

guess=a;

options=optimset('Display','off');

res=1;

while res>1e-4;

    [delta res]=fminsearch(@QF,guess,options,delta_d,delta_p,delta_h,solubility,n);

    guess=delta;

end

d_d=delta(1); d_p=delta(2); d_h=delta(3); R_o=delta(4);

R_a=sqrt(4*(d_d-delta_d).^2 + (d_p-delta_p).^2 + (d_h-delta_h).^2);

RED=(R_a/R_o);

clc

disp('*****')

disp('Delta_d Delta_p Delta_h Solub RED')

```

```
disp('*****')
```

```
disp([delta_d' delta_p' delta_h' solubility' RED'])
```

```
disp('Data Fit==')
```

```
Data_Fit=1+QF(delta,delta_d,delta_p,delta_h,solubility,n);
```

```
disp(Data_Fit)
```

```
disp('Delta_d Delta_p Delta_h R_o')
```

```
disp([d_d d_p d_h R_o])
```

Appendix B.

%%

%%

%%

%%

%% Matlab code for Calculation RED, Distance, d_d , d_p and d_h %%%

%%

%%

%%

clc

clear all

data = xlsread('DataS.xlsx'); %import data from excel file

delta_s = (data(:,4))'; %solvents used in swelling test

delta_d = (data(:,1))'; %solvents used in swelling test

delta_p = (data(:,2))'; %solvents used in swelling test

delta_h = (data(:,3))'; %solvents used in swelling test

```
n = 13; %number of solvents
```

```
ddT= 15.22; dpT= 16.18; dhT= 1.97 ; rT= 16.63; % Target solvent
```

```
SS1 = 100:-10:0;
```

```
SS2 = abs (100-SS1);
```

```
j1=1;
```

```
for i = 1:n;
```

```
    j2=1;
```

```
    for j=1:n;
```

```
        j3=1;
```

```
        for ii=1:1:11
```

```
            dd (i,j,ii)= ((SS1(ii) * delta_d(i))+ (SS2(ii)* delta_d(j)))/100;
```

```
            dp (i,j,ii)= ((SS1(ii) * delta_p(i))+ (SS2(ii)* delta_p(j)))/100;
```

```
            dh (i,j,ii)= ((SS1(ii) * delta_h(i))+ (SS2(ii)* delta_h(j)))/100;
```

```
            Distance (i,j,ii) = sqrt(4*(dd(i,j,ii) - ddT)^2 + (dp(i,j,ii) - dpT)^2+(dh(i,j,ii) - dhT)^2);
```

```
            RED (i,j,ii)= (Distance (i,j,ii) / rT);
```

```

        j3=j3+1;

    end

    j2=j2+1;

end

    j1=j1+1;

end

xlswrite('OutPutRED.xls',RED(:,1),'Sheet1','B2'); % Write data

xlswrite('OutPutRED.xls',RED(:,2),'Sheet2','B2'); % Write data

xlswrite('OutPutRED.xls',RED(:,3),'Sheet3','B2'); % Write data

xlswrite('OutPutRED.xls',RED(:,4),'Sheet4','B2'); % Write data

xlswrite('OutPutRED.xls',RED(:,5),'Sheet5','B2'); % Write data

xlswrite('OutPutRED.xls',RED(:,6),'Sheet6','B2'); % Write data

xlswrite('OutPutRED.xls',RED(:,7),'Sheet7','B2'); % Write data

xlswrite('OutPutRED.xls',RED(:,8),'Sheet8','B2'); % Write data

xlswrite('OutPutRED.xls',RED(:,9),'Sheet9','B2'); % Write data

xlswrite('OutPutRED.xls',RED(:,10),'Sheet10','B2'); % Write data

xlswrite('OutPutRED.xls',RED(:,11),'Sheet11','B2'); % Write data

```

%%

%%

xlswrite('OutPutDis.xls',Distance(:,1),'Sheet1','B2'); % Write data

xlswrite('OutPutDis.xls',Distance(:,2),'Sheet2','B2'); % Write data

xlswrite('OutPutDis.xls',Distance(:,3),'Sheet3','B2'); % Write data

xlswrite('OutPutDis.xls',Distance(:,4),'Sheet4','B2'); % Write data

xlswrite('OutPutDis.xls',Distance(:,5),'Sheet5','B2'); % Write data

xlswrite('OutPutDis.xls',Distance(:,6),'Sheet6','B2'); % Write data

xlswrite('OutPutDis.xls',Distance(:,7),'Sheet7','B2'); % Write data

xlswrite('OutPutDis.xls',Distance(:,8),'Sheet8','B2'); % Write data

xlswrite('OutPutDis.xls',Distance(:,9),'Sheet9','B2'); % Write data

xlswrite('OutPutDis.xls',Distance(:,10),'Sheet10','B2'); % Write data

xlswrite('OutPutDis.xls',Distance(:,11),'Sheet11','B2'); % Write data

%%

%%

xlswrite('OutPutdd.xls',dd(:,1),'Sheet1','B2'); % Write data

xlswrite('OutPutdd.xls',dd(:,2),'Sheet2','B2'); % Write data

```
xlswrite('OutPutdd.xls',dd(:,3),'Sheet3','B2'); % Write data
```

```
xlswrite('OutPutdd.xls',dd(:,4),'Sheet4','B2'); % Write data
```

```
xlswrite('OutPutdd.xls',dd(:,5),'Sheet5','B2'); % Write data
```

```
xlswrite('OutPutdd.xls',dd(:,6),'Sheet6','B2'); % Write data
```

```
xlswrite('OutPutdd.xls',dd(:,7),'Sheet7','B2'); % Write data
```

```
xlswrite('OutPutdd.xls',dd(:,8),'Sheet8','B2'); % Write data
```

```
xlswrite('OutPutdd.xls',dd(:,9),'Sheet9','B2'); % Write data
```

```
xlswrite('OutPutdd.xls',dd(:,10),'Sheet10','B2'); % Write data
```

```
xlswrite('OutPutdd.xls',dd(:,11),'Sheet11','B2'); % Write data
```

```
%%%%%%%%%%%%%%%%%%%%%%%%%%%%%%%%%%%%%%%%%%%%%%%%%%%%%%%%%%%%%%%%%%%%%%%%%
```

```
%%%%%%%%%%%%%%%%%%%%%%%%%%%%%%%%%%%%%%%%%%%%%%%%%%%%%%%%%%%%%%%%%%%%%%%%%
```

```
xlswrite('OutPutdp.xls',dp(:,1),'Sheet1','B2'); % Write data
```

```
xlswrite('OutPutdp.xls',dp(:,2),'Sheet2','B2'); % Write data
```

```
xlswrite('OutPutdp.xls',dp(:,3),'Sheet3','B2'); % Write data
```

```
xlswrite('OutPutdp.xls',dp(:,4),'Sheet4','B2'); % Write data
```

```
xlswrite('OutPutdp.xls',dp(:,5),'Sheet5','B2'); % Write data
```

```
xlswrite('OutPutdp.xls',dp(:,6),'Sheet6','B2'); % Write data
```

```
xlswrite('OutPutdp.xls',dp(:,7),'Sheet7','B2'); % Write data
```

```
xlswrite('OutPutdp.xls',dp(:,8),'Sheet8','B2'); % Write data
```

```
xlswrite('OutPutdp.xls',dp(:,9),'Sheet9','B2'); % Write data
```

```
xlswrite('OutPutdp.xls',dp(:,10),'Sheet10','B2'); % Write data
```

```
xlswrite('OutPutdp.xls',dp(:,11),'Sheet11','B2'); % Write data%
```

```
%%%%%%%%%%%%%%%%%%%%%%%%%%%%%%%%%%%%%%%%%%%%%%%%%%%%%%%%%%%%%%%%%%%%%%%%%
```

```
%%%%%%%%%%%%%%%%%%%%%%%%%%%%%%%%%%%%%%%%%%%%%%%%%%%%%%%%%%%%%%%%%%%%%%%%%
```

```
xlswrite('OutPutdh.xls',dh(:,1),'Sheet1','B2'); % Write data
```

```
xlswrite('OutPutdh.xls',dh(:,2),'Sheet2','B2'); % Write data
```

```
xlswrite('OutPutdh.xls',dh(:,3),'Sheet3','B2'); % Write data
```

```
xlswrite('OutPutdh.xls',dh(:,4),'Sheet4','B2'); % Write data
```

```
xlswrite('OutPutdh.xls',dh(:,5),'Sheet5','B2'); % Write data
```

```
xlswrite('OutPutdh.xls',dh(:,6),'Sheet6','B2'); % Write data
```

```
xlswrite('OutPutdh.xls',dh(:,7),'Sheet7','B2'); % Write data
```

```
xlswrite('OutPutdh.xls',dh(:,8),'Sheet8','B2'); % Write data
```

```
xlswrite('OutPutdh.xls',dh(:,9),'Sheet9','B2'); % Write data
```

```
xlswrite('OutPutdh.xls',dh(:,10),'Sheet10','B2'); % Write data
```



```
xlswrite('OutPutdh.xls',dh(:,11),'Sheet11','B2'); % Write data
```

```
%%%%%%%%%%%%%%%%%%%%%%%%%%%%%%%%%%%%%%%%%%%%%%%%%%%%%%%%%%%%%%%%%%%%%%%%
```

```
%%%%%%%%%%%%%%%%%%%%%%%%%%%%%%%%%%%%%%%%%%%%%%%%%%%%%%%%%%%%%%%%%%%%%%%%
```

```
%%%%%%%%%
```

```
%%%%%%%%%
```

```
%%%%%%%%%
```

Function

```
%%%%%%%%%
```

```
%%%%%%%%%
```

```
%%%%%%%%%
```

```
%%%%%%%%%%%%%%%%%%%%%%%%%%%%%%%%%%%%%%%%%%%%%%%%%%%%%%%%%%%%%%%%%%%%%%%%
```

```
%%%%%%%%%%%%%%%%%%%%%%%%%%%%%%%%%%%%%%%%%%%%%%%%%%%%%%%%%%%%%%%%%%%%%%%%
```

```
function y = QF(x,delta_d,delta_p,delta_h,solubility,n)
```

```
d_d=x(1);
```

```
d_p=x(2);
```

```
d_h=x(3);
```

```
R_o=x(4);
```

```
R_a=sqrt(4*(d_d-delta_d).^2 + (d_p-delta_p).^2 +(d_h-delta_h).^2);
```

```
for i=1:n,
```

```

if R_a(i)>R_o;

    if solubility(i)==0;

        A(i)=1;

    else

        A(i)=exp(R_o-R_a(i));

    end

else R_a(i)<R_o;

    if solubility(i)==0;

        A(i)=exp(R_a(i)-R_o);

    else

        A(i)=1;

    end

end

end

y=abs(((prod(A))^(1/n))-1);

```